Title: Spinal Mechanisms in Post-Activation Potentiation: Facilitation of Presynaptic Inhibition Contrasts H-Reflex Amplitude Reduction

*Miloš Kalc[1,2], Aleš Holobar[3], Matej Kramberger[3], Nina Murks[3], *Jakob Škarabot[2]

[1] Institute for Kinesiology Research, Science and Research Centre of Koper, Koper, Slovenia

[2] School of Sport, Exercise and Health Sciences, Loughborough University, Loughborough, UK

[3] System Software Laboratory, Faculty of Electrical Engineering and Computer Science, University of Maribor, Maribor, Slovenia

[1]Corresponding authors:

milos.kalc@zrs-kp.si

j.skarabot@lboro.ac.uk

* The authors are co-corresponding authors

Abstract

This study investigated the spinal neural mechanisms underlying post-activation potentiation in ten healthy young males (21.9 ± 4.8 years). Participants performed a 10-second maximal isometric plantarflexion, after which we measured twitch torque and assessed spinal excitability using the soleus H-reflex, D1 presynaptic inhibition and heteronymous Ia facilitation (HF). High-density surface EMG was decomposed to track single motor unit responses. The conditioning contraction increased twitch torque by 12.2 Nm ($p < 0.001$) immediately and returning to baseline within nine minutes. This mechanical potentiation was accompanied by a 29% reduction in H-reflex amplitude ($p < 0.001$), which recovered within three minutes. Paradoxically, neurophysiological indices of presynaptic inhibition, D1 and HF were significantly increased (D1: $p<0.017$; HF: $p<0.001$), resulting in spinal facilitation. Single MU analysis revealed increased discharge probability, particularly in higher-threshold units indicating overall spinal facilitation. These results demonstrate that post-activation potentiation involves a complex dissociation: H-reflex pathway inhibition along with facilitation of presynaptic spinal mechanisms. This paradox can be explained by either post-activation depression (caused by depletion of neurotransmitter at the Ia–motoneuron synapse) or muscle thixotropy, a contraction history-dependent decrease in muscle spindle sensitivity, which reduces the efficacy of the Ia afferent volley independently of spinal inhibitory mechanisms. Our findings highlight a dissociation between spinal presynaptic facilitation and the decreased H-reflex, underscoring the need for future studies to explicitly test the roles of post-activation depression and muscle thixotropy after conditioning contractions.

New & Noteworthy:

This study provides evidence that post-activation potentiation is accompanied by a reduction in soleus H-reflex amplitude and a concurrent facilitation of presynaptic spinal mechanisms. By combining global EMG and single motor unit analyses extracted from high-density surface EMG, we reveal a dissociation between spinal disinhibition and reflex depression. These findings suggest that acute post-contraction reflex suppression might be mediated by mechanisms other than presynaptic inhibition, potentially involving post-activation depression or changes in muscle spindle sensitivity.

Key words:

HDsEMG, Ia afference, soleus, heteroniumous Ia facilitation, spinal reflex

Introduction

Muscle contraction history significantly influences subsequent muscle contractions, which can either be enhanced or depressed. For example, electrically elicited tetani or short-lasting (<10 s) voluntary conditioning contractions (1) temporarily increase single-twitch performance. This phenomenon, known as post-activation potentiation (PAP) (2), is primarily influenced by the intensity and duration of the conditioning contraction (1). The principal mechanism behind the observed twitch potentiation is the phosphorylation of the regulatory myosin light chain (3). This phosphorylation alters myosin head orientation, enhancing the likelihood of force-generating cross-bridge interactions by reducing the distance to actin-binding sites (4). As a result, Ca^{2+} sensitivity is increased, making twitch force production more pronounced, particularly at lower contraction intensities, where Ca^{2+} levels are submaximal and the contractile apparatus is not yet saturated. Indeed, some studies have reported twitch force increases up to 200% immediately following a conditioning contraction (5), with potentiation tapering off exponentially over 10 minutes.

Although the primary mechanisms of PAP are well-established, emerging evidence suggests that neural processes could also contribute (6,7). However, the precise nature of neural contribution is equivocal, with studies showing Hoffmann reflex (H-reflex) depression (lateral gastrocnemius, LG: Güillich and Schmidtbleicher 2006; soleus, SOL: Enoka et al., 1980), enhancement (LG: Güillich and Schmidtbleicher 2006; SOL: Güillich and Schmidtbleicher 2006; Trimble and Harp 1998; vastus medialis: Folland et al. 2008), or no change (12–14) following a conditioning contraction (see Zero & Rice, 2021 for a comprehensive review). These discrepancies likely stem from variations in participant characteristics, the nature of the conditioning contractions, time of assessment relative to conditioning contraction, H-reflex assessment methods, muscle selection, and training status (e.g., enhancement more likely shown in trained athletes: Güillich (15), Folland (11)).

Because reflex potentiation tends to emerge several minutes after a conditioning contraction, while twitch potentiation typically dissipates more rapidly, some have argued that the delayed reflex effects are not directly related to PAP that mainly contributes to immediate increases in twitch force (16). Instead, they may reflect post-activation performance enhancement (PAPE) (3), which typically arises 5 to 10 minutes after a contraction, and encompasses improvements in neuromuscular function not directly linked to myosin regulatory light chain phosphorylation, such as elevated muscle temperature, fluid shifts, or increased blood flow. However, the early H-reflex depression has been linked more closely to PAP and is thought to reflect a compensatory neural strategy, possibly aimed at offsetting the enhanced muscle output (3), but the underlying mechanisms remain experimentally unverified.

A fundamental challenge in interpreting H-reflex changes lies in disentangling presynaptic (e.g., presynaptic inhibition) from postsynaptic (e.g., motoneuron excitability, reciprocal inhibition) mechanisms (17). To address this, electrophysiological techniques often employ conditioning stimuli, such as low-intensity volleys to antagonistic nerves, which elicit D1 (5–30 ms) and D2 (70–200 ms) inhibition responses largely attributed to presynaptic inhibition of Ia terminals (18). However, this approach has known limitations: postsynaptic effects may temporally overlap with presynaptic inhibition, while long-latency cutaneous facilitation or shifts in motor unit recruitment thresholds may confound interpretation by mimicking or masking true presynaptic changes (19). To resolve these ambiguities, Hultborn and colleagues (19) demonstrated that, within the first ~0.6 ms of the H-reflex response, monosynaptic Ia excitation remains uncontaminated by disynaptic inputs, making this early window a reliable indicator of pure Ia excitatory postsynaptic potentials (EPSPs). In principle, the most robust way to distinguish changes in presynaptic inhibition from postsynaptic motoneuron recruitment gain is through peri-stimulus time histogram (PSTH) analysis of single motor unit (MU)

discharges, which reflects the direct timing and probability of motoneuron activation in response to synaptic input. Although recent advances in high-density surface electromyography (HDsEMG) decomposition now allow the extraction of single MU responses during evoked contractions (20–23), this approach requires the delivery of a large number of stimuli, typically several tens to construct reliable PSTHs, making it impractical for studies of acute phenomena like PAP, where the time window for capturing spinal adaptations is limited to a few minutes. To address this constraint, we propose to assess the heteronymous Ia femoral facilitation (24,25), which in combination with D1 presynaptic inhibition assessment offers a more time-efficient method that allows a robust indirect quantification of presynaptic inhibitory effects on soleus Ia terminals.

In this study, we aimed to investigate the immediate and short-term neuromuscular responses following a maximal voluntary isometric conditioning contraction. Specifically, we examined the twitch force response and H-reflex amplitude, while also exploring potential contributions from presynaptic spinal mechanisms. Furthermore, leveraging a recently developed methodology to extract single MU discharges from HDsEMG signals in evoked contractions (20,21,23), we investigated how MU discharge patterns and amplitude cancellation may influence the observed H-reflex responses. Given the involvement of recreationally active participants in this study, we hypothesised that the conditioning contraction would immediately but transiently increase twitch torque and concurrently decrease the H-reflex amplitude, with reflex responses returning to baseline within approximately five minutes. With respect to presynaptic spinal mechanisms, we further hypothesised that presynaptic inhibition would be reduced following the conditioning contraction, potentially contributing to the observed changes in H-reflex amplitude.

Methods

Procedures

Participants

Ten young adult males (age 21.9 ± 4.8 years) participated in a single visit counterbalanced crossover repeated measures study. All participants were physically active at least 3-times per week with no history of neurological disorders or major lower-extremity neuromuscular injury as determined by a health history questionnaire (Par-Q; Thomas et al., 1992). Participants were instructed to avoid the consumption of caffeinated beverages and strenuous physical activity 24 hours before the experimental session. Each participant was briefed about any potential risks and discomfort they might face, and they provided written informed consent prior to involvement in the study. This research complied with the most recent principles outlined in the Declaration of Helsinki (except for registration in database), and it received clearance from the Research Ethics Committee of Slovenia (n 0120-84/2020/4).

Study design

Participants first visited the laboratory for a familiarisation session, during which they were acquainted with the electrical stimulation paradigms used in the study. They returned three to seven days later for the experimental session. The session began with a standardised warm-up consisting of isometric plantarflexion contractions lasting 4–6 seconds at 50% (2 repetitions), 60% (2x), 70% (1x), 80% (1x), and 90% (1x) of the participant's maximal perceived effort. This was followed by a torque-tracking preliminary procedure (see *Torque tracking preliminary procedure*). Subsequently, stimulation parameters for the tibial, common peroneal, and femoral nerves were determined. A 20-minute washout period was then introduced to reduce potential residual effects of the contractions on subsequent measurements.

During the experiment, participants were instructed to remain seated in the ankle dynamometer and perform one of two interventions: (i) a 10-second maximal voluntary isometric contraction (EXP), or (ii) passive rest (CON). Following each intervention, mechanical and electrophysiological responses to stimulation were recorded over an 18-minute period at 1, 3, 5, 7, 9, 12, 15, and 18-minutes post-intervention. This design, omitting baseline assessments prior to the intervention, was adapted from previous work (11,14). A 20-minute washout period was included between the two conditions to minimise carryover effects. The warm-up was repeated 10 minutes before the second intervention. Intervention order was counterbalanced across participants to reduce potential order effects. All testing was conducted in a temperature-controlled room maintained between 22 and 24 °C. A schematic representation of the intervention timeline is shown in Figure 1A.

Participant positioning

Participants were seated upright in the custom ankle dynamometer with their hips, knees, and ankles flexed at 90° (180° = full extension), consistent with prior studies examining PAP (14). The right leg was used for all measurements. The foot was strapped securely over the metatarsal region onto the footplate, with the lateral malleolus aligned with the device's axis of rotation (Figure 1C). A rigid support was placed over the thigh, just above the knee, to limit unwanted movement during plantarflexion. Participants rested their forearms on the device's arm supports and were instructed to maintain a relaxed posture. To reduce variability in spinal responses, participants were asked to keep their gaze fixed on a monitor in front of them, maintain a neutral head position, and avoid clenching their jaw or squeezing their hands during stimulation (27).

*** FIGURE 1 ABOUT HERE ***

Torque tracking preliminary procedure

Following the warm-up, participants rested for 60 seconds before performing two maximal voluntary isometric contractions (MVCs), separated by 120 seconds of rest. They were instructed to contract as fast and as hard as possible and maintain maximal effort for approximately 3 seconds. Strong verbal encouragement was provided to ensure maximal effort (28). After MVC determination, participants completed submaximal isometric contractions lasting 20 seconds at 10%, 20%, and 30% MVC, and 15 seconds at 40%, 50%, and 70% MVC. Each contraction was followed by a 120-second rest period to prevent fatigue. These torque-tracking contractions were used to establish MU separation filters, facilitating MU identification during electrically elicited contractions (20,23), see 'HDsEMG processing' section for details.

Conditioning contraction

Participants were instructed to contract their plantar flexors as fast and as hard as possible and maintain maximal effort for 10 seconds. Strong verbal encouragement was provided to ensure maximal effort (28). As indicated above, this was performed after a 20-minute washout period following either the torque-tracking preliminary procedure or the other condition (EXP or CON, as per randomisation).

Electromyographic recordings

Electromyographic signals were recorded from the soleus (SOL) muscle using both high-density surface EMG and bipolar EMG (biEMG). Prior to electrode placement, the skin over the SOL region was shaved and abraded with abrasive paste (29). The electrode array was mounted on the muscle belly covering the central portion of the soleus muscle, with the long side of the array aligned with the longitudinal axis of the muscle (Figure 1C). This electrode position has been suggested as the position where the H reflex with the largest amplitude can be observed on the soleus muscle (30). The biEMG electrodes were positioned laterally to the array, with a reference electrode positioned over the tibial tuberosity, and a ground electrode wrapped around the ankle. The HDsEMG was used to extract individual motor unit spike trains from both voluntary and evoked contractions, whereas the biEMG setup allowed for real-time monitoring of short signal segments (30 ms before to 70 ms after each electrical stimulus), ensuring visual feedback of the evoked responses and signal quality. The SOL was selected as the target muscle for EMG recordings because it allows for the assessment of multiple spinal inhibitory and facilitatory mechanisms via established H-reflex conditioning protocols (18,31).

Posterior tibial nerve stimulation

H-reflexes, M-waves, and mechanical twitches were elicited in the right soleus (SOL) muscle using single rectangular pulses (1 ms duration) delivered to the posterior tibial nerve. The stimulation anode was placed over the patella, while the optimal site for cathodal stimulation in the popliteal fossa was first identified using a stimulation pen and then marked for electrode placement.

To obtain the H-reflex and M-wave (HM) recruitment curve, stimulation began at 5 mA and was progressively increased in 1 mA steps until the maximal H-reflex amplitude (H_{MAX}) was reached. Once the H-reflex began to decline, stimulation intensity was further increased in 5 mA increments until no further increase in M-wave amplitude was observed. To ensure supramaximal stimulation, the final intensity was increased by 50%. These supramaximal stimuli (stimulation current: 92.7 ± 9.9 mA) were used to evoke maximal twitch peak torque (PT) and maximal M-wave (H_{MAX}).

To investigate the different spinal pathways after the interventions, the H-reflex was conditioned with nerve stimulations of homonymous spinal pathways to assess changes in the level of presynaptic inhibition acting on Ia afferent terminals. Unconditioned H-reflexes served as a baseline for conditioned volleys arising from i) stimulation of the common peroneal nerve to elicit presynaptic inhibition (D1) and ii) stimulation of the heteronymous nerve (femoral nerve) to elicit heteronymous Ia facilitation pathways (HF). Additionally, a mini recruitment curve was used to determine changes in maximal H-reflex post-intervention. A block of 16 stimuli (Figure 1B), comprising four unconditioned H-reflexes, four stimuli each for assessing D1 and HF, and four with progressively increasing intensity for H_{MAX}, were delivered at 6-second interstimulus intervals (Figure 1E).

Unconditioned H-reflex

To evoke the unconditioned SOL H-reflexes, the tibial nerve was stimulated with an intensity that induced a response of the SOL H-reflex in the ascending part of the HM recruitment curve (28.1 ± 6.0 mA) preceded by a visible small M-wave (M_{atH}) of amplitude between 5 and 10% of M_{MAX} (18). The

reproducibility of M_{atH} was used to monitor the stability and reliability of the stimulation. A stable M_{atH} indicates that a constant number of motor nerve fibres and Ia afferents are excited by the same stimuli, ensuring the consistency of stimulus condition within the experimental session (32). Thus, the intensity was slightly adjusted during the experiment to elicit a consistent M_{atH} amplitude. The peak-to-peak amplitude of the unconditioned H-reflex (H_{PTP}) was further considered in data analysis.

Assessment of D1 presynaptic inhibition

H-reflexes were conditioned to induce D1 presynaptic inhibition of Ia afferents onto α-motoneurons, following the methodology presented by Knikou (18). Conditioning stimuli, consisting of triplets at 300 Hz (1 ms width), were delivered to the branch of the common peroneal nerve activating ipsilateral pretibial flexors. Electrical stimulation was delivered with an intensity set at 1.2 times the motor threshold of the tibialis anterior (TA; Achache et al., 2010). Optimal conditioning-test timing for maximal H-reflex inhibition was determined for each participant at the start of the session, exploring intervals from 25 ms to 10 ms in 1 ms steps. The timing producing the highest inhibition was used. The ratio between the conditioned (D1) and the unconditioned reflex (H_{PTP}) indicates the activation of presynaptic inhibitory mechanisms (see Figure 1D) and was further considered in data analysis.

Assessment of Heteronymous Ia Facilitation

To examine HF, a conditioning stimulus was applied to the ipsilateral femoral nerve (Figure 1E). Single stimulations (1 ms pulse width) were set at 1.3 times the motor threshold of the vastus lateralis muscle. The most effective conditioning test interval for facilitating soleus HF amplitude was identified early in the experimental session, with intervals ranging from -10 ms to +5 ms in 1 ms steps. The timing that produced the highest facilitation in each participant was used. Special attention was given to the conditioning-test interval to ensure monosynaptic interaction of quadriceps Ia afferents with the triceps surae motoneuronal pool (34), as facilitations at larger intervals might also involve polysynaptic circuits. Bergmans et al. (35), have noted that heteronymous Ia facilitation of the H-reflex is not always observable in the lower limbs of all participants. Therefore, only participants who exhibited an increase in SOL H-reflex after a heteronymous conditioning impulse to the femoral nerve in familiarisation were invited to participate in the experimental session. The ratio between the conditioned (HF) and the unconditioned reflex (H_{PTP}) indicates the facilitation of the SOL Ia–α motoneuron after femoral nerve activation (Hultborn et al., 1987; Figure 1D) and was further considered in data analysis.

Maximal H-reflex amplitude

The maximal H-reflex was evoked by four stimuli starting at an intensity of 2 mA below the H_{MAX} reached at the beginning of the visit (1 mA increments). The H-reflex response that produced the highest peak-to-peak amplitude (stimulation current: 37.0 ± 9.5 mA) of the series of 4 stimuli was considered H_{MAX} for that time point.

Stimulation protocol justification

The stimulation protocol for studying spinal mechanisms in this study involved balancing the need for a sufficiently long inter-stimuli interval to prevent homosynaptic depression (36) in a resting muscle and the need for a significant number of stimuli to counteract the intrinsic variability of H-reflex amplitude (37). Though longer intervals (~10 s) are crucial to reduce homosynaptic depression risk (36,38,39), and 5 to 10 stimuli are typically needed to obtain a reliable measure of the physiological response (17), we aimed to record as many responses as feasible within a limited timeframe (90 s), targeting 16 stimuli divided into four groups. During the familiarization session, we experimented with shortening the inter-stimuli interval to determine the shortest possible duration without inducing homosynaptic depression. A 6-second interval emerged as the optimal compromise, as the

shortest duration not triggering homosynaptic depression in our participants, thereby allowing for a greater number of stimuli within the given timeframe.

Instrumentation

Isometric dynamometer

Isometric plantarflexion torque was recorded using a custom-made ankle dynamometer (Wise Technologies, Ljubljana, Slovenia). A load cell (Z6FC3/200kg, AEP transducers, Modena, Italy) was embedded in the footplate to measure plantarflexion torque.

Electromyography systems

HDsEMG signals were recorded using a semi-disposable adhesive electrode array with 5 columns × 13 rows and 8 mm interelectrode distance (GR08MM1305, OT Bioelettronica, Torino, Italy). Signals were amplified with a 16-bit amplifier (Quattrocento, OT Bioelettronica) and acquired at 5,120 Hz using OTBiolab+ software. A reference electrode (5 × 3 cm, T3545) was placed on the tibial tuberosity, and grounding was achieved using a water-soaked strap (WS2, OT Bioelettronica, Torino, Italy) around the ankle. Signals were band-pass filtered between 10–500 Hz.

Bipolar EMG signals were recorded with surface electrodes (Covidien 24 mm, interelectrode distance 25 mm) placed lateral to the HDsEMG array. The reference electrode (50 × 100 mm, 00734, Compex, UK) was placed over the patella. Signals were sampled at 10,000 Hz using PowerLab hardware and LabChart software (ADInstruments, Australia) and band-pass filtered (10–500 Hz).

Electrical stimulation equipment

The posterior tibial nerve was stimulated using a custom build constant-current stimulator (Stim_1, EMF Furlan, Ljubljana, Slovenia) delivering 1 ms rectangular pulses. The anode (50 × 90 mm, MyoTrode PLUS, Globus, Italy) was placed over the patella, and the cathode (25 mm diameter, J10R00, Axelgaard) over the popliteal fossa.

The common peroneal and femoral nerves were stimulated using the Digitimer DS7R stimulator (Digitimer, UK). Two silver chloride electrodes (8 mm) were placed over the upper anterolateral leg, distal to the fibular head to stimulate the common peroneal nerve. For femoral nerve stimulation, the cathode (25 mm diameter, J10R00, Axelgaard Manufacturing Co., Lystrup, Denmark) was placed in the femoral triangle and the anode (50 × 90 mm, MyoTrode PLUS, Globus, Italy) under the gluteus maximus. A manual switch was used to alternate stimulation targets.

Data processing

Global EMG.

EMG reflex responses were extracted from the array electrode. Two sets of five neighbouring monopolar signals within the central portion of the HDsEMG (columns 2–4 and rows 4–7 of the bidimensional array) were averaged and differentiated to obtain a bipolar EMG derivation with an equivalent interelectrode distance of 1.6 cm (40,41). Although EMG measurements were also taken in a bipolar configuration, we chose to extract the data from the array electrode because the H-reflex amplitude can vary substantially depending on the recording electrode's position (30), and because we aimed to obtain both global EMG and decomposed EMG from the same source.

Maximal M peak-to-peak amplitudes (M_{MAX}) were extracted from supramaximal stimulations. Following recent H-reflex reporting guidelines by Theodosiadou et al. (17), various parameters were extracted from the reflex electrophysiological response, including normalized peak-to-peak amplitude

(H_{PTP}/M_{MAX}), reflex latency (H_{LAT}), and duration (H_{DUR}) (Figure 1D). Additionally, to study D1 presynaptic inhibition and HF, we calculated the amplitude ratios of D1 and HF conditioned reflexes to their respective unconditioned responses: $D1/H_{PTP}$ and HF/H_{PTP}.

Torque data

Torque signals were filtered with a low-pass fourth-order zero-lag Butterworth filter at a cutoff frequency of 25 Hz. From these filtered signals, the peak twitch torque (TW_{PT}) was calculated for the supramaximal stimulations.

HDsEMG processing

An extended explanation of the procedure involved in the detection of single MUs discharges during elicited contractions can be found in our previous works (20,21,23). Briefly, HDsEMG signals were decomposed using the well-established Convolution Kernel Compensation (CKC) algorithm (42). First, data from isometric torque tracking contractions collected at the beginning of the experimental session (see '*Torque tracking preliminary procedure*') were decomposed for each contraction level in isolation (Figure 2A and 2B). The decomposition's effectiveness was quantitatively evaluated using the Pulse-to-Noise Ratio (PNR), which is a reliable indicator of the motor unit (MU) identification precision (43). Any MUs with a PNR below 28 dB were excluded from further analysis. The firing patterns of the remaining MUs underwent meticulous scrutiny and refinement by an expert. This editing process involved discarding MUs that exhibited fewer than 5 consecutive firings, unusually low instantaneous firing rates (<4 Hz), or highly variable firing patterns, as indicated by a coefficient of variation of the interspike interval exceeding 0.4 (44). For each MU that passed these criteria, its respective MU filter was determined. This filter denotes the specific linear combination of spatio-temporal HDsEMG channel data that approximates the spike train of an individual MU (42,45). Notably, in situations involving isometric muscle contractions, an MU filter derived from signals of one contraction can be applied effectively to signals of another contraction of the same muscle to ascertain the corresponding MU spike train (42,45). In our experiment, we initially established MU filters from voluntary contraction HDsEMG signals and then applied these filters to the HDsEMG signals of elicited H-reflexes. To avoid redundancy in MU identification across different levels of voluntary contraction, the firing patterns of MUs were compared against each other. Any duplicates identified (i.e., MUs sharing more than 30% of their firings), were removed by retaining only the ones with the highest PNR, thereby ensuring the uniqueness of each MU in the analysis. Subsequently, these refined MU filters were applied to the HDsEMG signals from H-reflexes, facilitating the identification of MU spike trains in evoked contractions (Figure 2C). The identified MU spike trains were segmented into actual MU discharges or baseline noise, an approach inherent to the CKC method (42). The final step involved a meticulous manual review by an expert, who compared the presence of crosstalk in MU spike trains derived from both voluntary and evoked contractions, making manual adjustments to the segmentation results where necessary, as suggested previously (43,45–47). It is important to note that only MUs identified in the isometric contractions could be detected in electrically evoked contractions. Moreover, recruitment threshold was estimated as the instantaneous torque at the instant of the first spike in the binary spike train during voluntary contractions.

Following MUs identification, we extracted the MU firing Latencies (HMU_{LAT}, $D1MU_{LAT}$, $HFMU_{LAT}$, $H_{MAX}MU_{LAT}$) and probability of MU discharge (HMU_{PROB}, $D1MU_{PROB}$, $HFMU_{PROB}$, $H_{MAX}MU_{PROB}$).

MU discharge ratio was calculated between recognized and discharged MUs for conditioning responses. $D1_{TO}HMU_{RATIO}$ and $HF_{TO}HMU_{RATIO}$ were calculated subtracting the unconditioned H reflex discharge ratio from D1 and HF discharge ratios, respectively. This metric was calculated to compare single MU data to $D1/H_{PTP}$ and HF/H_{PTP} extracted from global EMG.

In addition, electrically elicited responses generate MU discharges that are highly synchronous; however, axonal conduction velocities, recruitment thresholds, and the spatial distribution of innervation zones introduce small but systematic differences in MUAP latency (23). MU synchronisation was thus quantified using two complementary measures: (1) the standard deviation of MU firing latencies, and (2) compound motor unit action potential (CMAP) amplitude cancellation. The temporal dispersion of MU discharges was quantified as the *standard deviation* of MU firing latencies for each reflex response. This measure was computed for all evoked responses (HMU_{SD}, $D1MU_{SD}$, $HFMU_{SD}$, $H_{max}MU_{SD}$) and reflects the spread of MU discharges around the mean response latency. CMAP amplitude cancellation arises from the algebraic summation of the positive and negative phases of MUAPs (48) for each reflex response. When MU discharges occur with temporal dispersion, simultaneous summation becomes less constructive, and the resulting compound waveform exhibits a reduced amplitude. Thus, greater cancellation indicates lower synchrony, whereas lower cancellation reflects highly synchronous MU firing (Figure 2E). To quantify cancellation, we computed two versions of the CMAP for each reflex response: $CMAP_{REAL}$ - the summation of MUAPs obtained using the actual MU discharge latencies, and $CMAP_{ALIGNED}$ - the summation of MUAPs obtained after temporal alignment of all MUAPs at their positive peak, creating an idealised condition of zero temporal dispersion and therefore minimal cancellation. The amplitude cancellation index was then defined in Equation 1:

$$CMAP_{CANC} = \frac{CMAP_{REAL}}{CMAP_{ALIGNED}}$$

Equation 1: $CMAP_{CANC}$ represents CMAP amplitude cancellation, calculated as the ration between $CMAP_{REAL}$ - the arithmetic summation of MUAPS aligned using their true discharging latencies and $CMAP_{ALIGNED}$ the summation of the same MUPAS aligned at their peak values.

Importantly, although MUAP shape strongly influences amplitude cancellation under typical circumstances *(48)*, this does not pose a methodological limitation here because both $MUAP_{REAL}$ and $MUAP_{ALIGNED}$ are constructed from the same set of MUAPs; therefore, any shape-related factor cancels out, and the ratio isolates only temporal dispersion. However, other limitations of CMAP amplitude cancellation-based metrics may bias the results. Indeed, CMAP amplitude cancellation depends on the number of MU discharges *(48)*. This phenomenon particularly affects the results of this study, because cancellation becomes ill-defined when only one or very few MU discharges are present in a single reflex response, causing the cancellation to approach higher values. We addressed this issue by analysing the impact of the number of discharging MUs on CMAP amplitude cancellation and reporting our mitigation procedure in the Supplemental Figure S1.

Please note that the per-MU analyses served as a complementary approach to our primary global EMG analysis. Because meaningful changes in the global EMG were observed only in the early post-intervention period, MU-level analyses were restricted to the first four time points.

***** FIGURE 2 ABOUT HERE *****

Statistical analysis

Statistical analyses were performed using the R programming language (v.4.2.1; R Foundation for Statistical Computing, Vienna, Austria) within the RStudio environment (2025.09.2). Linear and generalized linear mixed-effects models were used to evaluate changes in neurophysiological and mechanical outcomes, with *lme4* (49) and *lmerTest* (50) packages.

To assess the effect of intervention (EXP vs. CON) and timepoint (eight levels) on torque (TW_{PT}), a set of global EMG outcomes (peak-to-peak amplitude, latency, and duration of reflex responses), and a set of outcomes calculated from the combined discharges of all MUs within each evoked response (MU discharge ratio, MU discharge standard deviation and CMAP amplitude cancellation), linear mixed-effects models were fitted with *intervention*, *timepoint*, and their interaction as fixed effects. Participant ID were included as random intercepts, with intervention also modelled as a random slope:

$$Outcome \sim Intervention \times Timepoint + (1 + Intervention \mid Participant\ ID)$$

MU-level data were extracted only from the first four timepoints. For MU outcomes based on individual firings (MU discharge probabilities and MU latencies), models were extended to include standardised MU R*ecruitment Threshold* as a continuous covariate. Two-way interactions between R*ecruitment Threshold* and both *intervention* and *timepoint* were included:

$$Outcome \sim Intervention \times Timepoint + Recruitment\ Threshold : Intervention + Recruitment\ Threshold : Timepoint + (1 + Intervention \mid Participant\ ID)$$

MU discharge probability, a binary outcome (1 = MU discharged; 0 = MU not discharged), was analysed using a generalized linear mixed model (GLMM) with a *binomial* distribution and *logit* link function in the *lme4* package. Although a logistic link was used, estimated marginal means are reported as predicted probabilities, not odds ratios, to aid interpretation.

Model assumptions (e.g., normality of residuals and random effects, homogeneity of variance, linearity, and multicollinearity) were verified using the *performance* package (51). All models were analysed separately for each elicited response condition: H, H_{MAX}, D1 and HF.

Post hoc interaction contrasts and simple effects were tested using the *emmeans* package (52), with p-values adjusted using the *multivariate t* method (53). For torque and global EMG data, the 8th timepoint was used as the reference level for comparisons; for MU-based data, the 4th timepoint served as the reference. Estimated marginal means and 95% confidence intervals were reported for all outcomes, while trends of the continuous covariate are presented graphically. The significance threshold for all analyses was set at $\alpha = 0.05$. Cohen's *d* effect sizes were calculated as the difference between estimated marginal means divided by the residual standard deviation of the fitted model. Effect size thresholds were interpreted as: $d < 0.2$ negligible, $d < 0.5$ small, $d < 0.8$ medium, and $d \geq 0.8$ large (54).

Results

Torque results

TW_{PT} was significantly affected by *time × intervention* interaction ($F_{7,\ 146.07} = 27.21$; $p < 0.001$), with interaction contrasts revealing differential modulation of TW_{PT} between interventions at 1, 3, 5 and 7 compared to 18 minutes after contraction ($p < 0.001$; $d = 4.89$; $p < 0.001$, $d = 2.01$; $p < 0.001$, $d = 1.85$; $p = 0.005$, $d = 1.41$, respectively (Figure 3C). Simple contrasts revealed that TW_{PT} in the EXP condition were 12.2 Nm ($p < 0.001$, $d = 4.71$), 4.73 Nm ($p = 0.002$, $d = 1.83$), 4.30 Nm ($p = 0.004$, $d = 1.66$) and 3.18 Nm ($p = 0.028$, $d = 1.23$) higher compared to CON conditions at 1, 3, 5, and 7 minutes after intervention, respectively.

M_{MAX} was not significantly affected by the interaction between *time × intervention* ($F_{7,\ 135} = 1.50$, $p = 0.169$, Figure 3D).

435 ***** FIGURE 3 ABOUT HERE *****

436

437 ## Global EMG results

438 H_{PTP}/M_{MAX} was significantly affected by the interaction between *time × intervention* ($F_{7, 496.03} = 3.38$, p
439 < 0.003), with interaction contrasts revealing modulation of H_{PTP}/M_{MAX} between interventions at 1
440 compared to 18 minutes after contraction (p = 0.002; d = 3.60; Figure 4Figure 4D). Simple contrasts
441 revealed that in H_{PTP}/M_{MAX} in the EXP condition was 29.3 percentage points (p < 0.001, d = 3.13) lower
442 compared to CON conditions at 1 minutes after contraction.

443 $D1/H_{PTP}$ and HF/H_{PTP} were significantly affected by the interaction between *time × intervention* ($F_{7,}$
444 $_{567.13} = 3.70$, p < 0.001 and $F_{7, 437.33} = 4.99$, p < 0.001, respectively), with interaction contrasts revealing
445 modulation in both variables between interventions at 1 compared to 18 minutes after contraction (p
446 = 0.017, d = 0.71, Figure 4D; and p < 0.001, d = 1.15, Figure 4E, respectively). Simple contrasts
447 revealed that in $D1/H_{PTP}$ and HF/H_{PTP} in the EXP condition were 17.1 (p < 0.017, d = 0.57) and 28
448 percentage points (p < 0.001, d = 1.25) higher compared to CON conditions 1 minute after
449 intervention. CON condition remained statistically unchanged for the whole duration of the
450 experiment (p ≥ 0.154).

451 H_{LAT}, H_{DUR}, H_{MAX}, were not significantly affected by the interaction between *time × intervention* (H_{LAT}:
452 $F_{6, 18.12} = 0.95$, p = 0.481; H_{DUR}: $F_{7, 64.82} = 0.38$, p = 0.923; H_{MAX}: $F_{7, 136.00} = 1.45$, p = 0.190, Figure 4B;
453 respectively).

454

455 ***** FIGURE 4 ABOUT HERE *****

456

457 ## Single motor unit behaviour results

458 A total of 537 MUs resulting in 53.7 ± 16.9 (range 21-78) unique MUs per participant were detected
459 (Table 1). The latencies of MU discharges were not significantly affected by the interaction between
460 *time × intervention* in any of the assessed conditioning protocols (HMU_{LAT}: $F_{45112.7} = 0.99$, p = 0.396;
461 $D1MU_{LAT}$: $F_{3, 4573.3} = 1.31$, p = 0.267; $HFMU_{LAT}$: $F_{3, 5660} = 0.48$, p = 0.692; $H_{MAX}MU_{LAT}$: $F_{3, 6428.6} = 1.02$, p =
462 0.378; Figure 5B). However, MU discharge latencies were strongly dependent on MU *recruitment*
463 *threshold* (HMU_{LAT}: $F_{1, 5117} = 21.1$, p < 0.001; $D1MU_{LAT}$: $F_{1, 4547.3} = 10.49$, p = 0.001; $HFMU_{LAT}$: $F_{1, 5655} =$
464 34.06, p < 0.001; $H_{MAX}MU_{LAT}$: $F_{1, 6426.5} = 29.22$, p < 0.001), with higher-threshold MUs exhibiting longer
465 latencies (Figure 5C). Moreover, a significant *intervention × recruitment threshold* interaction
466 emerged for $D1MU_{LAT}$ ($F_{1, 4392.3} = 4.23$, p = 0.039), where the EXP condition showed a reduced
467 influence of recruitment threshold on MU firing latency.

468

469 *Table 1: Descriptive statistics of recognized and discharged Motor Units*

	n	Mean ± SD / person [range]
Recognised MUs	556	55.6 ± 16.6 [21 - 78]
Discharged MUs / response		21.8 ± 13.9 [0 - 64]

470

*** FIGURE 5 ABOUT HERE ***

MU discharge probability showed a significant interaction between *time × intervention* in all assessed conditioning protocols (HMU_{PROB}: $\chi^2_3 = 38.09$, $p < 0.001$; $D1MU_{PROB}$: $\chi^2_3 = 27.15$, $p < 0.001$; $HFMU_{PROB}$: $\chi^2_3 = 57.80$, $p < 0.001$; $H_{max}MU_{PROB}$: $\chi^2_3 = 50.04$, $p < 0.001$; Figure 6A). Moreover, a significant *intervention × recruitment threshold* interaction emerged for all conditioning protocols (HMU_{PROB}: $\chi^2_4 = 206.80$, $p < 0.001$; $D1MU_{PROB}$: $\chi^2_4 = 214.267$, $p < 0.001$; $HFMU_{PROB}$: $\chi^2_4 = 152.67$, $p < 0.001$; $H_{max}MU_{PROB}$: $\chi^2_4 = 115.13$, $p < 0.001$), showing higher probability of MU discharge in higher-threshold MUs in the EXP condition (Figure 6B).

MU discharge ratio was not significantly affected by the interaction between *time × intervention* in any of the assessed conditioning protocols ($D1_{TO}HMU_{RATIO}$: $F_{3\ 49.93} = 1.18$, $p = 0.324$; $HF_{TO}HMU_{RATIO}$: $F_{3\ 50.58} = 1.26$, $p = 0.295$).

CMAP amplitude cancellation for $HCMAP_{CANC}$ and $H_{MAX}CMAP_{CANC}$ were significantly affected by the interaction between *time × intervention* ($F_{3,\ 205.33} = 3.32$, $p = 0.020$ and $F_{3,\ 157.19} = 4.13$, $p = 0.007$, respectively; Figure 6C). However, interaction contrasts showed no difference between interventions in any timepoint for $HCMAP_{CANC}$ (Figure 6D), whereas $H_{MAX\text{-}CANC}$ demonstrated a significant difference between 1 and 7 minutes ($p = 0.008$, $d = 0.89$). No significant *time × intervention* interaction was found for $D1_{CANC}$ and HF_{CANC} ($F_{3,\ 163.68} = 0.74$, $p = 0.524$ and $F_{3,\ 224.18} = 2.52$, $p = 0.058$, respectively).

The *standard deviation* of MU discharges were not significantly affected by the interaction between *time × intervention* in any of the assessed conditioning protocols (HMU_{SD}: $F_{3,\ 223.15} = 0.49$, $p = 0.687$; $D1MU_{SD}$: $F_{3,\ 217.1} = 2.17$, $p = 0.113$; $HFMU_{SD}$: $F_{3,\ 227} = 0.25$, $p = 0.854$; $H_{max}MU_{SD}$: $F_{1,\ 199.88} = 1.42$, $p = 0.235$).

*** FIGURE 6 ABOUT HERE ***

*** FIGURE 7 ABOUT HERE ***

Discussion

This study aimed to investigate the immediate and short-term neuromuscular responses following a maximal voluntary isometric conditioning contraction. Specifically, we assessed the muscle's mechanical (single twitch) and neurophysiological (H-reflex) response, with the aim of elucidating the role of presynaptic spinal mechanisms. The main findings indicate that a brief maximal isometric conditioning contraction led to an increase in twitch torque, accompanied by a diminished H-reflex amplitude, which occurred despite indicators of reduced presynaptic inhibitory spinal mechanisms, as evidenced by increased D1 and HF responses. Modulation of mechanical and neurophysiological responses was transient in nature, vanishing after nine and three minutes after contraction,

respectively. To the best of our knowledge, this is the first study to specifically examine spinal presynaptic mechanisms in the context of PAP.

The pattern of mechanical and neurophysiological responses following a strong conditioning contraction

TW_{PT} was increased immediately after the conditioning contraction and persisted for about 9 minutes, demonstrating a strong potentiation effect, in line with previous studies investigating PAP (5,11,14). Concomitantly, M_{MAX} remained unaffected by any intervention, consistent with a prior study (11), suggesting that sarcolemmal membrane excitability was not affected by the conditioning contraction (55). Conversely, H_{PTP} was significantly decreased immediately following the conditioning contraction, but returned to baseline within three minutes. The decreased H_{PTP} immediately post-conditioning contraction is consistent with some studies (9,10,15) but not others (Folland et al., 2008; Iglesias-Soler et al., 2011; Wallace et al., 2019), with the discrepancies between studies possibly attributed to variations in training status, conditioning contraction duration, intensity, type, and involved body region, as well as differences in the H-reflex methodology. Regarding the latter, studies interchangeably used the maximal H-reflex and H-reflex measured on the ascending part of the HM recruitment curve (Trimble & Harp (1998); like H_{PTP} used in this study). Indeed, in our study H_{PTP} significantly decreased, whereas the H_{MAX} remained statistically unchanged. While the lack of observed changes in H_{MAX} might also be due to the timing of the stimulation (i.e., the effect might have dissipated by the time H_{MAX} was assessed in our protocol), recent findings suggest that the maximal H-reflex may lack sensitivity to inhibitory mechanisms, potentially obscuring key physiological insights (17).

Prior studies have also reported an increase in reflex amplitude between 4 and 11 minutes after the contraction (8,11), an effect not observed in our study. According to a recent review (3) the delayed reflex potentiation reported in some studies might not be attributable to PAP, but to PAPE, a neuromechanical potentiation associated with mechanisms unrelated to PAP, such as increased muscle temperature, water content, and blood flow (16). Furthermore, we can exclude changes in the onset of the reflex responses in the motoneuron or changes in the synchronisation of MU firings as the likely mechanisms for the observed H-reflex depression, due to no significant changes in unconditioned and conditioned H-reflex latencies (H_{LAT}); (Knikou & Rymer, 2002) and no differences in the duration of the H-reflex (H_{DUR}), respectively.

In previous studies, the drop in H_{PTP} immediately after conditioning contraction was suggested to be a compensatory mechanism to accommodate the enhanced muscular response (3), however, the direct effect of enhanced muscle contractile properties to the spinal excitability is still unknown. In our data, H_{PTP} amplitude was decreased concomitantly with TW_{PT} increase only at the first timepoint, suggesting that other mechanisms contribute to the neural modulation observed following the conditioning contraction. Similarly, the acute depression of the H-reflex amplitude is not always found during PAP (12–14).

Moreover, it is important to consider the specific characteristics of SOL when interpreting the relationship between spinal responses and twitch potentiation in the present study. SOL is composed predominantly of slow-twitch muscle fibres (approx. 80%) (57), which are less susceptible to potentiation than fast-twitch fibres (58,59). Consequently, it is reasonable to suggest, that spinal mechanisms associated with PAP in SOL might be less pronounced compared to muscles with a higher proportion of fast-twitch fibres. Furthermore, although the knee was flexed during testing to reduce the mechanical contribution of the gastrocnemii to plantar flexion torque, the tibial nerve stimulation used to elicit twitches and H-reflexes innervates the entire triceps surae. The

gastrocnemius muscles, which contain a relatively greater proportion of fast-twitch muscle fibres (approx. 40%) (57), likely contributed substantially to the twitch torque measured, and may therefore account for a considerable portion of the observed potentiation. As such, linking the magnitude of plantar flexor twitch potentiation exclusively to SOL-level spinal adaptations should be interpreted with caution. However, SOL remains the preferred muscle for examining spinal inhibitory and facilitatory mechanisms in humans, providing a methodological window that is not readily available in the gastrocnemii.

The role of presynaptic mechanisms in H-reflex reduction following a conditioning contraction

Contrary to our hypothesis, we observed significant increases in presynaptic inhibition-related parameters D1/H_{PTP} and HF/H_{PTP}. Thus, changes of D1/H_{PTP} and HF/H_{PTP} suggest spinal facilitation or disinhibition rather than inhibition. This indicates a complex interplay between inhibitory and facilitatory spinal mechanisms following voluntary contractions and supports the idea that mechanisms other than presynaptic inhibition influence the observed reduction in H_{PTP}. Observations from animal studies show that a short conditioning contraction elevates the transmittance of excitation potentials across synaptic junctions at the spinal cord (37,60), which can explain the observed disinhibition/facilitation of D1/H_{PTP} and HF/H_{PTP}. An induced tetanic contraction has been suggested to decrease the transmitter failure during subsequent activity, via one or a combination of several possible responses, including an increase in the quantity of neurotransmitter released, an increase in the efficacy of the neurotransmitter, or a reduction in axonal branch-point failure along the afferent neural fibres (60,61). Moreover, consistent with our findings, following a conditioning contraction in the upper limbs that induced PAP, several studies reported reduced cervicomedullary motor evoked potential amplitude that has a large monosynaptic component and is generally not influenced by presynaptic inhibition (62,63).

Another possible explanation for the drop in H_{PTP} observed in our study is the involvement of post-activation depression (PAD), a mechanism often attributed to the depletion of neurotransmitter release at the synaptic cleft due to previous activation of Ia afferents (38). PAD is known to be attenuated during sustained contractions, possibly due to enhanced Ia firing induced by the voluntary contraction (31,64). In this context, the soleus and gastrocnemius lateralis H-reflex were found to be less depressed immediately after the conditioning contraction when assessed during a sustained voluntary contraction compared to rest, which was interpreted as evidence of PAD-induced depression of the H reflex amplitude (Xenofondos et al. (7)).

The transient reduction in H_{PTP} observed in the present study could also be explained by a rapid, history-dependent decrease in the sensitivity of muscle spindle Ia afferents, a peripheral phenomenon known as muscle thixotropy (65). After the conditioning contraction, the muscle fibres, having formed stable cross-bridges at a shortened length, would be in a slack state at the testing position. While the presence of slack in the whole muscle may not always be apparent, the intrafusal fibres of the muscle spindles with their compliant connections to adjacent extrafusal fibres are particularly prone to slack (66), which dramatically reduces tension on the spindle's sensory endings, lowering their baseline discharge rate. This is supported by data in cats, where a conditioning contraction has been shown to dramatically reduce discharge rate of primary muscle spindle endings (from 40 to 10 pps), suggesting a profound, momentary desensitization of the sensory part of the muscle spindle without any change in actual muscle length (67). In the case of our study, the standardised submaximal stimulus that activates the axons originating from spindles will have evoked a less synchronous or less potent volley of action potentials arriving at the spinal cord, leading to

weaker excitatory post-synaptic potential generated by the alpha motoneuron when the spindle axons will have been in a thixotropic, low-sensitivity state after a conditioning contraction, resulting in decreased H-reflex. Indeed, the human evidence supports this supposition, showing that conditioning contractions that alter muscle thixotropy can modulate H-reflex amplitude (68). Although postsynaptic mechanisms such as post-activation depression represent a possible explanation for the apparent contradiction in in our data (i.e. decreased H-reflex with presynaptic inhibition measures pointing toward facilitation), thixotropy offers an additional plausible explanation where the decreased H-reflex reflects a peripheral decrease in Ia-afferent efficacy rather than a change in spinal inhibition. Future studies designed to directly assess post activation depression and presynaptic inhibition while manipulating muscle thixotropy (e.g., via specific conditioning contractions) are needed to test this hypothesis explicitly.

Effects of a conditioning contraction on spinal mechanisms gleaned from single motor units

Additional insights into the effects induced by a conditioning contraction on spinal mechanisms were obtained through the decomposition of the HDsEMG signals into contributions of individual MUs. MU discharge latency was not affected by the conditioning contraction, confirming the results observed from global EMG metrics. Moreover, the MU discharge probability was similar between conditions immediately after the conditioning contraction. However, discharge probability increased three minutes after the contraction in the EXP compared to the CON condition across all stimulation paradigms and was significantly higher in higher-threshold MUs. This observation is in line with animal studies where tetanic contraction decreased the transmitter failure occurring primarily at larger motoneurons, which resulted in a considerable potentiation effect in these motoneurons (60). In addition, CMAP amplitude cancellation, a measure of MU discharge synchronisation, was lower in the EXP condition, suggesting increased synchronisation of MU discharges following the conditioning contraction. Overall, the combination of lower CMAP amplitude cancellation and higher discharge probability, particularly in higher-threshold units, suggests that the conditioning contraction induced facilitation rather than inhibition. These results contradict the reflex amplitude metrics observed at the global EMG level (H_{PTP}), not only in the direction of change but also in timing. Specifically, MU-level differences emerged three minutes after the contraction, whereas the decrease in H_{PTP} occurred immediately. Moreover, these results are in contrast with the observations in studies investigating contraction history effects on voluntary contractions, where an increase in muscle contraction capacity was accompanied by a decrease in MU discharge rate, without clear additional recruitment of MUs to compensate for the discharge rate loss (69,70).

When interpreting the discrepancy between single MU variables and global EMG metrics reported in this study, it is important to note that MU discharge probability metrics do not represent a fair comparison to $D1_{PTP}/H_{PTP}$ and HF_{PTP}/H_{PTP} which are normalized to the H_{PTP} amplitude. Thus, we computed the $D1_{TO}H_{RATIO}$ and $HF_{TO}H_{RATIO}$, where we subtracted the number of discharged MUs in the unconditioned contraction from D1 and HF, respectively, and expressed this difference as a ratio with respect to the total identified MUs of each participant. The analysis of the discharge ratio shows that analysis at the MU level also captures the pattern of D1 inhibition and HF facilitation, which can be seen as a decrease or increase in $D1_{TO}H_{RATIO}$ and $HF_{TO}H_{RATIO}$, respectively. However, discharge ratio was not sufficiently sensitive to capture the increase in D1 and HF, as seen in the global EMG ($D1_{PTP}/H_{PTP}$ and HF_{PTP}/H_{PTP}). In this respect, it is important to acknowledge that HDsEMG decomposition captures only a subset of active MUs, with a bias toward larger and more superficial units (46), whereas global EMG provides a more integrated representation of the whole muscle (71). Furthermore, amplitude metrics from global EMG are continuous and non-affected by single-unit errors, whereas MU-level analyses rely on a relatively small number of units and discharges. As such, mislabelling or missing a

few MU discharges can disproportionately influence the results. Though the single MU analysis provided complementary evidence to increased spinal excitability following voluntary contraction particularly in higher-threshold units, future studies employing a higher stimulus count are warranted to fully exploit the potential of this method for detailed mapping of motoneuron pool adaptations.

The role of spinal mechanisms with respect to the reported effects of conditioning contraction on MU discharge rate in submaximal voluntary contractions

The increased per-MU discharge probability observed in the present study, derived from H-reflex measures and therefore reflecting the excitability of spinal circuits in response to electrically evoked input, should be contextualised within the broader literature on voluntary MU control when the muscle is in a potentiated state. It has been consistently shown that during voluntary isometric contractions at low to moderate intensities (≤75% MVC), MU firing rates are reduced when the muscle is potentiated following a conditioning contraction (69,70,72,73). Interestingly, MU discharge rate is highly responsive to changes in muscle contractile state induced by potentiation and/or sustained contraction, making rapid compensatory discharge rate adjustments (increasing/decreasing discharge rate) dependent on the active state of the muscle. This compensatory mechanism has been speculated to be partially mediated by group III and IV afferents, providing mechanical and metabolic feedback from the muscle to the CNS, as well as by Golgi tendon organs (GTO) conveying tendon tension information via Ib afferents (69,70). In this regard, musculo-tendinous stiffness has been suggested to increase following a conditioning contraction (see Blazevich and Babault 2019 for a comprehensive review), which could be detected by GTOs and subsequently influence spinal excitability via Ib afferent pathways. However, recent work by Zero and Rice (74) demonstrated that the reduction in voluntary firing rates following a conditioning contraction could be primarily attributable to a decrease in voluntary descending drive rather than to peripheral afferent feedback from the potentiated muscle per se (74). When visual torque feedback was withheld and participants targeted the same submaximal force level, no modification in MU firing rates or rating of perceived exertion occurred despite the muscle being in a potentiated state; instead, torque output was overestimated by approximately 50% (74). This indicates that the motoneuron is not directly sensitised to alterations in the active state of the muscle through peripheral feedback, and that compensatory adjustments in neural output arise from reductions in voluntary descending input driven by visual task demands.

It is therefore important to distinguish between the excitability of spinal circuits as assessed by electrically evoked measures (such as the H-reflex and per-MU discharge probability reported here) and MU discharge behaviour during voluntary contractions, which additionally reflects the magnitude of voluntary descending drive and task-specific sensory feedback. While the present findings suggest that spinal circuitry is in a facilitated state following the conditioning contraction, the net outcome during voluntary submaximal control is a clear reduction in MU firing rates (73). Whether the spinal adaptations reported here (reduced presynaptic inhibition and enhanced heteronymous facilitation) are part of the same compensatory process that permits lower voluntary drive to sustain a given torque output, or represent a distinct and parallel mechanism, remains an open question.

Limitations

This study presents several limitations. First, although the stimulation block intended to induce the H-reflex in the ascending part of the H/M recruitment curve, the D1, HF, and maximal H reflex blocks lasted 90 seconds, and only four stimuli were elicited per response. While 5–10 reflexes are typically

recommended for reliable assessment (17), the approach used in this study allowed us to examine multiple neurophysiological mechanisms within a single session with the low variability within each time point (Figure 4A) suggesting four stimuli were sufficient to capture the modulation.

Second, although similar intervals were used in prior work (13), we used a shorter interstimulus interval (6 seconds) than the 10 seconds typically recommended for resting H-reflex assessments to minimize post-activation depression (75). Varying intervals were tested during the pilot and familiarization phases, allowing us to identify the shortest interval that did not induce post-activation depression, thereby increasing the number of stimuli per block. Maximal twitches were elicited immediately after the conditioning contraction and could theoretically influence subsequent H reflexes. However, an identical stimulation paradigm was used in the CON condition, which did not show any decrease in H reflex amplitude, suggesting that prior maximal stimulations did not bias the reflex responses. The maximal H reflex was assessed 60 seconds after H_{PTP}, which may have allowed conditioning contraction-induced modulation to dissipate. Nonetheless, HF assessed just 20 seconds earlier remained significantly elevated, suggesting that the absence of H_{MAX} modulation more likely reflects a methodological limitation of H_{MAX}, rather than an absence of neurophysiological effects.

Furthermore, this study was conducted exclusively in males. Sex hormones fluctuate across the menstrual cycle and are known to modulate spinal excitability (76), and H-reflex parameters have been shown to differ between sexes even when hormone levels are comparable (77). Caution should therefore be exercised when generalizing these findings to female populations or to individuals experiencing hormonal changes across the lifespan. Future studies should examine whether the present findings extend to females.

MU-level analysis is biased by the small number of units identifiable within each evoked response. Although our group has previously demonstrated the feasibility of extracting MUs from evoked responses (20,21,23), achieving physiologically robust results still requires hundreds of responses. For example, in a recent study (22) we successfully used PSTHs to extract information from the earliest portion of the reflex response, which reflects the monosynaptic phase of Ia presynaptic inhibition (19). Although this analysis reinforced the physiological effects observed at the global EMG level, a greater number of evoked responses than the number used in the present study is required for HDsEMG-derived MU metrics to reach the reliability comparable to intramuscular EMG. Future attempts to apply similar techniques to study fast, transient neurophysiological phenomena such as PAP should consider incorporating low-intensity background muscle activity to reduce post-activation depression (a common limitation in resting H-reflex paradigms) and enable the acquisition of a much greater number of stimuli within a similar assessment window. This approach would strengthen the robustness of non-invasive spinal assessments and enhance the mechanistic insights available from PSTH/PSF analyses.

Finally, it is important to acknowledge that a maximal voluntary conditioning contraction may simultaneously induce contractile dysfunction alongside potentiation (78). These two processes share a common Ca^{2+}-dependency but operate through opposing mechanisms. Activity-dependent potentiation results from phosphorylation of the RLC, which increases the Ca^{2+} sensitivity of the contractile apparatus, enhancing force production at submaximal Ca^{2+} concentrations without altering maximal force (79,80). Contractile dysfunction as a result of a sustained contraction, by contrast, is primarily associated with a reduction in peak myoplasmic Ca^{2+} concentration due to inhibited release from the sarcoplasmic reticulum, impairing force production particularly at high frequencies (81) or decreased Ca^{2+} sensitivity (82). Because potentiation preferentially enhances force at low stimulation frequencies (single twitch), while contraction-induced contractile dysfunction impairs force at high frequencies (doublet or train), these two processes can coexist with opposing

effects at different points along the force-frequency relationship. However, our post-conditioning assessment relied exclusively on single electrically elicited twitches and H-reflexes, and thus any contractile dysfunction-related impairment at higher stimulation frequencies would not have been detectable with the methodology employed. Although previous studies employing a similar conditioning contraction reported no contractile dysfunction (69), whether the observed twitch potentiation reflects pure potentiation or a net outcome of coexisting potentiation and contraction-induced contractile dysfunction therefore remains unresolved. Future studies should incorporate a proper stimulations methodology to dissociate these effects.

Conclusions

This study offers novel insights into the neuromuscular responses following a maximal voluntary isometric conditioning contraction, particularly regarding spinal mechanisms. Our results indicate that a brief but intense voluntary contraction, enhances twitch torque, accompanied by a disinhibition (facilitation) of presynaptic inhibitory mechanisms, as shown by increased D1 and HF responses. The observed reduction in H reflex amplitude immediately after the contraction, however, suggests that additional spinal mechanisms or an intrinsic muscle contraction history-dependent mechanical state may modulate spinal output. Future studies should therefore dissociate spinal mechanisms from muscle thixotropy using protocols that isolate their independent effects.

SUPPLEMENTAL MATERIAL:

Supplemental Fig. S1: https://doi.org/10.17605/OSF.IO/78CDW

References

1. Vandervoort AA, Quinlan J, McComas AJ. Twitch potentiation after voluntary contraction. Exp Neurol. 1983 Jul;81(1):141–52. doi:10.1016/0014-4886(83)90163-2 PubMed PMID: 6861942.

2. Sale DG. Postactivation Potentiation: Role in Human Performance. Exercise and Sport Sciences Reviews. 2002 Jul;30(3):138. doi:10.1097/00003677-200207000-00008

3. Zero AM, Rice CL. State-of-the-art review: spinal and supraspinal responses to muscle potentiation in humans. Eur J Appl Physiol. 2021 May 1;121(5):1271–82. doi:10.1007/s00421-021-04610-x

4. Levine RJ, Kensler RW, Yang Z, Stull JT, Sweeney HL. Myosin light chain phosphorylation affects the structure of rabbit skeletal muscle thick filaments. Biophysical Journal. 1996 Aug;71(2):898–907. doi:10.1016/S0006-3495(96)79293-7

5. Baudry S, Duchateau J. Postactivation potentiation in human muscle is not related to the type of maximal conditioning contraction. Muscle & Nerve. 2004;30(3):328–36. doi:10.1002/mus.20101

6. Tillin NA, Bishop D. Factors modulating post-activation potentiation and its effect on performance of subsequent explosive activities. Sports Med. 2009;39(2):147–66. doi:10.2165/00007256-200939020-00004 PubMed PMID: 19203135.

7. Xenofondos A, Patikas D, Koceja DM, Behdad T, Bassa E, Kellis E, et al. Post-activation potentiation: The neural effects of post—activation depression. Muscle & Nerve. 2015;52(2):252–9. doi:10.1002/mus.24533

8. Güllich A, Sehmidtbleicher D. MVC-induced short- term potentiation of explosive force. In. 2006 [cited 2024 Mar 5]. Available from: https://www.semanticscholar.org/paper/MVC-induced-short-term-potentiation-of-explosive-G%C3%BCllich-Sehmidtbleicher/212432ded5f49d8d9e1d25bbcdba4d7fbf3c73f3

9. Enoka RM, Hutton RS, Eldred E. Changes in excitability of tendon tap and Hoffmann reflexes following voluntary contractions. Electroencephalogr Clin Neurophysiol. 1980 Jun;48(6):664–72. doi:10.1016/0013-4694(80)90423-x PubMed PMID: 6155255.

10. Trimble MH, Harp SS. Postexercise potentiation of the H-reflex in humans. Medicine & Science in Sports & Exercise. 1998 Jun;30(6):933–41.

11. Folland JP, Wakamatsu T, Fimland MS. The influence of maximal isometric activity on twitch and H-reflex potentiation, and quadriceps femoris performance. Eur J Appl Physiol. 2008 Nov;104(4):739–48. doi:10.1007/s00421-008-0823-6 PubMed PMID: 18665389.

12. Hodgson MJ, Docherty D, Zehr EP. Postactivation potentiation of force is independent of h-reflex excitability. Int J Sports Physiol Perform. 2008 Jun;3(2):219–31. doi:10.1123/ijspp.3.2.219 PubMed PMID: 19208930.

13. Iglesias-Soler E, Paredes X, Carballeira E, Márquez G, Fernández-Del-Olmo M. Effect of intensity and duration of conditioning protocol on post-activation potentiation and changes in H-reflex. European Journal of Sport Science. 2011;11(1):33–8. doi:10.1080/17461391003770517

14. Wallace BJ, Shapiro R, Wallace KL, Abel MG, Symons TB. Muscular and Neural Contributions to Postactivation Potentiation. The Journal of Strength & Conditioning Research. 2019 Mar;33(3):615–25. doi:10.1519/jsc.0000000000003011

15. Guellich A, Schmidtbleicher D. MVC-induced short-term potentiation of explosiv force. New Studies in Athletics. 1996 Jan 1;11:67–84.

16. Blazevich AJ, Babault N. Post-activation Potentiation Versus Post-activation Performance Enhancement in Humans: Historical Perspective, Underlying Mechanisms, and Current Issues. Front Physiol. 2019;10:1359. doi:10.3389/fphys.2019.01359 PubMed PMID: 31736781; PubMed Central PMCID: PMC6838751.

17. Theodosiadou A, Henry M, Duchateau J, Baudry S. Revisiting the use of Hoffmann reflex in motor control research on humans. Eur J Appl Physiol. 2022 Dec 26. doi:10.1007/s00421-022-05119-7

18. Knikou M. The H-reflex as a probe: pathways and pitfalls. Journal of neuroscience methods. 2008 Jun;171(1):1–12. doi:10.1016/j.jneumeth.2008.02.012 PubMed PMID: 18394711.

19. Hultborn H, Meunier S, Morin C, Pierrot-Deseilligny E. Assessing changes in presynaptic inhibition of I a fibres: a study in man and the cat. The Journal of Physiology. 1987;389(1):729–56. doi:10.1113/jphysiol.1987.sp016680

20. Kalc M, Škarabot J, Divjak M, Urh F, Kramberger M, Vogrin M, et al. Identification of motor unit firings in H-reflex of soleus muscle recorded by high-density surface electromyography. IEEE Transactions on Neural Systems and Rehabilitation Engineering. 2022;1–1. doi:10.1109/TNSRE.2022.3217450

21. Kalc M, Škarabot J, Divjak M, Urh F, Kramberger M, Vogrin M, et al. Motor unit identification in the M waves recorded by high-density electromyogram. IEEE Transactions on Biomedical Engineering. 2022;1–11. doi:10.1109/TBME.2022.3224962

22. Magdič M, Holobar A, Kramberger M, Vogrin M, Murks N, Fekonja A, et al. Acute effects of orofacial, neck, and shoulder relaxation exercises and chewing on soleus H-reflex and motor unit discharge patterns. Journal of Neurophysiology. 2025 Jun;133(6):1886–901. doi:10.1152/jn.00461.2024

23. Škarabot J, Ammann C, Balshaw TG, Divjak M, Urh F, Murks N, et al. Decoding firings of a large population of human motor units from high-density surface electromyogram in response to transcranial magnetic stimulation. The Journal of Physiology. 2023;601(10):1719–44. doi:10.1113/JP284043

24. Grosprêtre S, Gueugneau N, Martin A, Lepers R. Presynaptic inhibition mechanisms may subserve the spinal excitability modulation induced by neuromuscular electrical stimulation. J Electromyogr Kinesiol. 2018 Jun;40:95–101. doi:10.1016/j.jelekin.2018.04.012 PubMed PMID: 29705497.

25. Pierrot-Deseilligny E, Mazevet D. The monosynaptic reflex: a tool to investigate motor control in humans. Interest and limits. Neurophysiologie Clinique/Clinical Neurophysiology. 2000 Apr 1;30(2):67–80. doi:10/czj2mp

26. Thomas S, Reading J, Shephard RJ. Revision of the Physical Activity Readiness Questionnaire (PAR-Q). Can J Sport Sci. 1992 Dec;17(4):338–45. PubMed PMID: 1330274.

27. Mitsuyama A, Takahashi T, Ueno T. Effects of teeth clenching on the soleus H reflex during lower limb muscle fatigue. Journal of Prosthodontic Research. 2017 Apr;61(2):202–9. doi:10.1016/j.jpor.2016.05.003

28. Verges S, Maffiuletti N a, Kerherve H, Decorte N, Wuyam B, Millet GY. Comparison of electrical and magnetic stimulations to assess quadriceps muscle function. Journal of applied physiology (Bethesda, Md : 1985). 2009 Feb;106(2):701–10. doi:10.1152/japplphysiol.01051.2007 PubMed PMID: 18756009.

29. Piervirgili G, Petracca F, Merletti R. A new method to assess skin treatments for lowering the impedance and noise of individual gelled Ag-AgCl electrodes. Physiological measurement. 2014;35(10):2101–18. doi:10.1088/0967-3334/35/10/2101 PubMed PMID: 25243492.

30. Botter A, Vazzoler I, Vieira TM. High density EMG investigation of h-reflex distribution over the soleus muscle. In: 2015 37th Annual International Conference of the IEEE Engineering in Medicine and Biology Society (EMBC) [Internet]. Milan: IEEE; 2015 [cited 2020 Apr 14]. p. 3460–3. Available from: http://ieeexplore.ieee.org/document/7319137/ doi:10.1109/EMBC.2015.7319137

31. Burke D. Clinical uses of H reflexes of upper and lower limb muscles. Clin Neurophysiol Pract. 2016 Apr 7;1:9–17. doi:10.1016/j.cnp.2016.02.003 PubMed PMID: 30214954; PubMed Central PMCID: PMC6123946.

32. Grosprêtre S, Papaxanthis C, Martin A. Modulation of spinal excitability by a sub-threshold stimulation of M1 area during muscle lengthening. Neuroscience. 2014 Mar 28;263:60–71. doi:10.1016/j.neuroscience.2014.01.013 PubMed PMID: 24434774.

33. Achache V, Roche N, Lamy JC, Boakye M, Lackmy A, Gastal A, et al. Transmission within several spinal pathways in adults with cerebral palsy. Brain. 2010 May;133(Pt 5):1470–83. doi:10.1093/brain/awq053 PubMed PMID: 20403961.

34. Morita H, Shindo M, Yanagawa S, Yoshida T, Momoi H, Yanagisawa N. Progressive decrease in heteronymous monosynaptic Ia facilitation with human ageing. Exp Brain Res. 1995;104(1):167–70. doi:10.1007/BF00229867 PubMed PMID: 7621936.

35. Bergmans J, Delwaide PJ, Gadea-Ciria M. Short-latency effects of low-threshold muscular afferent fibers on different motoneuronal pools of the lower limb in man. Experimental Neurology. 1978 Jun;60(2):380–5. doi:10.1016/0014-4886(78)90091-2

36. Özyurt MG, Topkara B, Şenocak BS, Budan AS, Yüce MN, Türker KS. Post-activation depression of primary afferents reevaluated in humans. Journal of Electromyography and Kinesiology. 2020 Oct;54:102460. doi:10.1016/j.jelekin.2020.102460

37. Gossard JP, Floeter MK, Kawai Y, Burke RE, Chang T, Schiff SJ. Fluctuations of excitability in the monosynaptic reflex pathway to lumbar motoneurons in the cat. Journal of Neurophysiology. 1994 Sep;72(3):1227–39. doi:10.1152/jn.1994.72.3.1227

38. Hultborn H, Illert M, Nielsen J, Paul A, Ballegaard M, Wiese H. On the mechanism of the post-activation depression of the H-reflex in human subjects. Exp Brain Res. 1996 Mar;108(3):450–62. doi:10.1007/bf00227268 PubMed PMID: 8801125.

39. Stein RB, Estabrooks KL, McGie S, Roth MJ, Jones KE. Quantifying the effects of voluntary contraction and inter-stimulus interval on the human soleus H-reflex. Experimental brain research. 2007 Sep;182(3):309. doi:10.1007/s00221-007-0989-x PubMed PMID: 17562030; PubMed Central PMCID: PMC5005071.

40. Del Vecchio A, Negro F, Felici F, Farina D. Associations between motor unit action potential parameters and surface EMG features. Journal of Applied Physiology. 2017 Oct;123(4):835–43. doi:10.1152/japplphysiol.00482.2017

41. Del Vecchio A, Negro F, Felici F, Farina D. Distribution of muscle fibre conduction velocity for representative samples of motor units in the full recruitment range of the tibialis anterior muscle. Acta Physiologica. 2018;222(2):e12930. doi:10.1111/apha.12930

42. Holobar A, Zazula D. Multichannel Blind Source Separation Using Convolution Kernel Compensation. IEEE Trans Signal Process. 2007 Sep;55(9):4487–96. doi:10.1109/TSP.2007.896108

43. Holobar A, Farina D, Gazzoni M, Merletti R, Zazula D. Estimating motor unit discharge patterns from high-density surface electromyogram. Clinical Neurophysiology. 2009 Mar 1;120(3):551–62. doi:10.1016/j.clinph.2008.10.160

44. Drost G, Stegeman DF, van Engelen BGM, Zwarts MJ. Clinical applications of high-density surface EMG: a systematic review. J Electromyogr Kinesiol. 2006 Dec;16(6):586–602. doi:10.1016/j.jelekin.2006.09.005 PubMed PMID: 17085302.

45. Farina D, Negro F, Gazzoni M, Enoka RM. Detecting the Unique Representation of Motor-Unit Action Potentials in the Surface Electromyogram. Journal of Neurophysiology. 2008 Sep;100(3):1223–33. doi:10.1152/jn.90219.2008

46. Farina D, Holobar A, Merletti R, Enoka RM. Decoding the neural drive to muscles from the surface electromyogram. Clin Neurophysiol. 2010 Oct;121(10):1616–23. doi:10.1016/j.clinph.2009.10.040 PubMed PMID: 20444646.

47. Negro F, Muceli S, Castronovo AM, Holobar A, Farina D. Multi-channel intramuscular and surface EMG decomposition by convolutive blind source separation. J Neural Eng. 2016 Feb;13(2):026027. doi:10.1088/1741-2560/13/2/026027

48. Farina D, Cescon C, Negro F, Enoka RM. Amplitude Cancellation of Motor-Unit Action Potentials in the Surface Electromyogram Can Be Estimated With Spike-Triggered Averaging. Journal of Neurophysiology. 2008 Jul;100(1):431–40. doi:10.1152/jn.90365.2008

49. Bates D, Mächler M, Bolker B, Walker S. Fitting Linear Mixed-Effects Models using lme4 [Internet]. arXiv; 2014 [cited 2024 Apr 22]. Available from: http://arxiv.org/abs/1406.5823 doi:10.48550/arXiv.1406.5823

50. Kuznetsova A, Brockhoff PB, Christensen RHB. **lmerTest** Package: Tests in Linear Mixed Effects Models. J Stat Soft. 2017;82(13). doi:10.18637/jss.v082.i13

51. Lüdecke D, Ben-Shachar MS, Patil I, Waggoner P, Makowski D. performance: An R package for assessment, comparison and testing of statistical models. Journal of Open Source Software. 2021;6(60):3139. doi:10.21105/joss.03139

52. Lenth R, Singmann H, Love J, Buerkner P, Herve M. emmeans: Estimated Marginal Means, aka Least-Squares Means [Internet]. 2020 [cited 2018 Dec 29]. Available from: https://CRAN.R-project.org/package=emmeans

53. Genz A, Bretz F. Comparison of Methods for the Computation of Multivariate t Probabilities. Journal of Computational and Graphical Statistics. 2002 Dec 1;11(4):950–71. doi:10.1198/106186002394

54. Cohen J. Statistical power analysis for the behavioral sciences. Hillsdale, N.J.: L. Erlbaum Associates; 1988.

55. Rodriguez-Falces J, Place N. Sarcolemmal Excitability, M-Wave Changes, and Conduction Velocity During a Sustained Low-Force Contraction. Front Physiol. 2021 Oct 15;12. doi:10.3389/fphys.2021.732624

56. Knikou M, Rymer WZ. Hip angle induced modulation of H reflex amplitude, latency and duration in spinal cord injured humans. Clin Neurophysiol. 2002 Nov;113(11):1698–708. doi:10.1016/s1388-2457(02)00285-7 PubMed PMID: 12417222.

57. Gollnick PD, Sjödin B, Karlsson J, Jansson E, Saltin B. Human soleus muscle: A comparison of fiber composition and enzyme activities with other leg muscles. Pflugers Arch. 1974 Sep 1;348(3):247–55. doi:10.1007/BF00587415

58. Sweeney HL, Bowman BF, Stull JT. Myosin light chain phosphorylation in vertebrate striated muscle: regulation and function. American Journal of Physiology-Cell Physiology. 1993 May;264(5):C1085–95. doi:10.1152/ajpcell.1993.264.5.C1085

59. Vandenboom R, Grange RW, Houston ME. Threshold for force potentiation associated with skeletal myosin phosphorylation. American Journal of Physiology-Cell Physiology. 1993 Dec;265(6):C1456–62. doi:10.1152/ajpcell.1993.265.6.C1456

60. Lüscher HR, Ruenzel P, Henneman E. Composite EPSPs in motoneurons of different sizes before and during PTP: implications for transmission failure and its relief in Ia projections. Journal of Neurophysiology. 1983 Jan;49(1):269–89. doi:10.1152/jn.1983.49.1.269

61. Clamann HP, Mathis J, Luscher HR. Variance analysis of excitatory postsynaptic potentials in cat spinal motoneurons during posttetanic potentiation. Journal of Neurophysiology. 1989 Feb;61(2):403–16. doi:10.1152/jn.1989.61.2.403

62. Jackson A, Baker SN, Fetz EE. Tests for presynaptic modulation of corticospinal terminals from peripheral afferents and pyramidal tract in the macaque. The Journal of Physiology. 2006 May 15;573(1):107–20. doi:10.1113/jphysiol.2005.100537

63. Nielsen J, Petersen N. Is presynaptic inhibition distributed to corticospinal fibres in man? The Journal of Physiology. 1994;477(1):47–58. doi:10.1113/jphysiol.1994.sp020170

64. Burke D, Adams RW, Skuse NF. The effects of voluntary contraction on the H reflex of human limb muscles. Brain. 1989 Apr;112 (Pt 2):417–33. doi:10.1093/brain/112.2.417 PubMed PMID: 2706438.

65. Proske U, Morgan DL. Do cross-bridges contribute to the tension during stretch of passive muscle? J Muscle Res Cell Motil. 1999 Aug;20(5–6):433–42. doi:10.1023/a:1005573625675 PubMed PMID: 10555062.

66. Proske U, Morgan DL, Gregory JE. Thixotropy in skeletal muscle and in muscle spindles: a review. Prog Neurobiol. 1993 Dec;41(6):705–21. doi:10.1016/0301-0082(93)90032-n PubMed PMID: 8140258.

67. Gregory JE, Morgan DL, Proske U. Aftereffects in the responses of cat muscle spindles. Journal of Neurophysiology. 1986 Aug;56(2):451–61. doi:10.1152/jn.1986.56.2.451

68. Wood SA, Gregory JE, Proske U. The influence of muscle spindle discharge on the human H reflex and the monosynaptic reflex in the cat. J Physiol. 1996 Nov 15;497(Pt 1):279–90. doi:10.1113/jphysiol.1996.sp021767 PubMed PMID: 8951729; PubMed Central PMCID: PMC1160930.

69. Inglis JG, Howard J, McIntosh K, Gabriel DA, Vandenboom R. Decreased motor unit discharge rate in the potentiated human tibialis anterior muscle. Acta Physiologica. 2011;201(4):483–92. doi:10.1111/j.1748-1716.2010.02233.x

70. Klein CS, Ivanova TD, Rice CL, Garland SJ. Motor unit discharge rate following twitch potentiation in human triceps brachii muscle. Neuroscience Letters. 2001 Dec;316(3):153–6. doi:10.1016/S0304-3940(01)02389-8

71. Vieira TM, Botter A. The Accurate Assessment of Muscle Excitation Requires the Detection of Multiple Surface Electromyograms. Exercise and Sport Sciences Reviews. 2021 Jan;49(1):23. doi:10.1249/JES.0000000000000240

72. McKiel A, Woods S, Gabriel DA, Vandenboom R, Falk B. Post-activation potentiation and potentiated motor unit firing patterns in boys and men. Eur J Appl Physiol. 2024 May 1;124(5):1561–74. doi:10.1007/s00421-023-05377-z

73. Zero AM, Fanous J, Rice CL. Acute and prolonged competing effects of activation history on human motor unit firing rates during contractile impairment and recovery. J Physiol. 2023 Dec;601(24):5689–703. doi:10.1113/JP285189 PubMed PMID: 37962903.

74. Zero AM, Rice CL. Without visual feedback voluntary torque is overestimated during muscle potentiation despite similar motor unit firing rate and perception of exertion. Journal of Neurophysiology. 2025 Mar;133(3):775–83. doi:10.1152/jn.00450.2024

75. Palmieri RM, Ingersoll CD, Hoffman MA. The Hoffmann Reflex: Methodologic Considerations and Applications for Use in Sports Medicine and Athletic Training Research. J Athl Train. 2004;39(3):268–77. PubMed PMID: 16558683; PubMed Central PMCID: PMC522151.

76. Soedirdjo SDH, Chung YC, Dhaher YY. Sex hormone mediated change on flexion reflex. Front Neurosci. 2023 Dec 21;17. doi:10.3389/fnins.2023.1263756

77. Hoffman M, Norcross M, Johnson S. The Hoffmann reflex is different in men and women. Neuroreport. 2018 Mar 7;29(4):314–6. doi:10.1097/WNR.0000000000000961 PubMed PMID: 29293170.

78. Rassier DE, Macintosh BR. Coexistence of potentiation and fatigue in skeletal muscle. Braz J Med Biol Res. 2000 May;33(5):499–508. PubMed PMID: 10775880.

79. Persechini A, Stull JT, Cooke R. The effect of myosin phosphorylation on the contractile properties of skinned rabbit skeletal muscle fibers. J Biol Chem. 1985 Jul 5;260(13):7951–4. PubMed PMID: 3839239.

80. Sweeney HL, Stull JT. Phosphorylation of myosin in permeabilized mammalian cardiac and skeletal muscle cells. Am J Physiol. 1986 Apr;250(4 Pt 1):C657-660. doi:10.1152/ajpcell.1986.250.4.C657 PubMed PMID: 3754389.

81. Westerblad H, Duty S, Allen DG. Intracellular calcium concentration during low-frequency fatigue in isolated single fibers of mouse skeletal muscle. J Appl Physiol. 1993 Jul 1;75(1):382–8. doi:10.1152/jappl.1993.75.1.382

82. Allen DG, Lannergren J, Westerblad H. Muscle cell function during prolonged activity: cellular mechanisms of fatigue. Exp Physiol. 1995;80(4):497–527. doi:10.1113/expphysiol.1995.sp003864

Figure 1: Study design and schematic representation of the assessment procedures. A) Study timeline, including the pre-experiment phase and two experimental conditions (EXP and CON). Vertical arrows indicate the timing of supramaximal electrical stimulations, while the grey boxes represent the blocks of stimulations used to assess spinal reflexes. B) Detailed depiction of the stimulation block, consisting of one supramaximal stimulus (twitch, TW) and 16 submaximal stimuli. These stimuli are grouped in sets of four, designed to assess: H-reflex at the ascending part of the H-M recruitment curve (H), D1 presynaptic Ia inhibition, heteronymous Ia facilitation (HF), and a mini H-M recruitment curve to evaluate the maximal H-reflex. C) Illustration of the participant's posture on the ankle dynamometer and the points of H-reflex stimulation along the tibial nerve pathway and the placement of the electrode array. D) Representative examples of mechanical (torque) and electrophysiological (M-wave) responses to a single supramaximal stimulus (upper traces), and a typical H-reflex response to submaximal stimulation (lower trace), with key features extracted from the H-reflex waveform (peak-to-peak amplitude, latency, and duration). E) Schematic representations of the spinal circuits involved in different types of reflex modulation (from left to right): H-reflex, D1 presynaptic Ia inhibition, heteronymous Ia facilitation, and maximal H-reflex. The corresponding electrophysiological responses are shown for each reflex type.

Figure 2: Representative data from a participant and methodological steps to extract single motor unit firings from the HDsEMG recordings. A) Raw electrophysiological signal during a voluntary isometric contraction. B) Extracted motor unit firings during voluntary isometric contractions. C) Reflex response propagation on a sample of channels on an electrode array; D) MU firings extracted form a reflex response. E) Example of CMAP amplitude cancellation. Arithmetic summation of eight MUAPs using recorded latencies and aligned based on the positive peak amplitude, respectively. F) Graphical representation of MU firings extracted from the electrophysiological response in consecutive stimuli. Each panel represent the temporal distribution (latency) of MUs firings with different recruitment thresholds. G) Graphical representation of summated MU firings for the maximal H-reflex, H-reflex, D1 and HR responses, respectively. In the upper figure, the coloured squares represent firings latencies of motor units of different recruitment thresholds. Darker colour represents a higher firing count at same latency at a millisecond precision. The sum of same data is depicted in the histogram at the bottom with the respective global EMG reflex response. Note that the relationship between latencies and recruitment thresholds on the level of individual motor units might not be related, likely due to detection delays (23); however, at the level of the whole sample higher threshold MUs exhibited longer discharge latencies compared to lower-threshold MUs (see Results).

Figure 3: Mechanical and electrophysiological responses to supramaximal electrical stimulations. A) Torque responses over time from a representative participant, illustrating the modulation of torque traces across different time points. B) Representative M-wave responses over time. To facilitate comparison between conditions, traces from the EXP condition are time-shifted by 15 ms to avoid overlap. C) Maximal twitch peak torque across time points. D) Peak-to-peak M-wave amplitudes (MMAX). Statistical data are presented as estimated marginal means with 95% confidence intervals for both the control (CON, red circles) and experimental (EXP, blue triangles) conditions. Smaller and lighter colour circles and triangles represent individual raw data points. Horizontal lines represent

statistically significant interaction effects, accompanied by p values and Cohen d values above the relevant lines.

Figure 4: Global electrophysiological responses to submaximal electrical stimulations. A) Unconditioned (HPTP, HMAX) and conditioned (HD1, HHF) H-reflex responses over time from a representative participant, illustrating the modulation of electrophysiological responses across different time points. Thin line traces represent raw signals; meanwhile thick traces represent the mean response. Blue and red box in D1 and HF traces represent the amplitude of the unconditioned H-reflex in the same stimulation block for EXP and CON interventions, respectively, allowing for a visual comparison of the unconditioned and conditioned H-reflex amplitude. B) Maximal H-reflex peak-to-peak amplitude (HMAX) across time points. C) Unconditioned peak-to-peak amplitude of the H-reflex in the ascending part of the H/M recruitment curve (HPTP). D) Ratio between the conditioned (D1PTP) and unconditioned H-reflex (HPTP) peak-to-peak amplitudes. E) Ratio between the conditioned (HFPTP) and unconditioned H-reflex (HPTP) peak-to-peak amplitudes. Statistical data are presented as estimated marginal means with 95% confidence intervals for both the control (CON, red circles) and experimental (EXP, blue triangles) conditions. Smaller and lighter colour circles and triangles represent individual raw data points in the background. Horizontal lines represent statistically significant interaction effects, accompanied by p values and Cohen d values above the relevant lines.

Figure 5: Motor unit (MU) discharges in elicited contractions. A) Unconditioned (H, HMAX) and conditioned (D1, HF) H-reflex responses between 1 and 3 minutes after intervention and respective MU firings from a representative participant. EXP (blue) electrophysiological responses are shifted by 15 ms compared to CON (red) to avoid overlap. Vertical lines represent MU firings. B) MU latency across timepoints. C) Graphical representation of the influence of recruitment threshold on MU latency across timepoint and different stimulation conditions. Statistical data are presented as estimated marginal means with 95% confidence intervals for both the control (CON, red circles) and experimental (EXP, blue triangles) conditions. Smaller and lighter colour circles and triangles represent individual raw data points in the background. Horizontal lines represent statistically significant interaction effects, accompanied by p values and Cohen d values above the relevant lines.

Figure 6: Motor unit (MU) discharges in elicited contractions. A) MU discharge probability. B) Graphical representation of the influence of recruitment threshold on MU discharge probability. C) Difference between conditioned and unconditioned discharge rate. D) CMAP amplitude cancellation. Statistical data are presented as estimated marginal means with 95% confidence intervals for both the control (CON, red circles) and experimental (EXP, blue triangles) conditions. Smaller and lighter colour circles and triangles represent individual raw data points in the background. Horizontal lines represent statistically significant interaction effects, accompanied by p values and Cohen d values above the relevant lines.

Figure 7: Mean standard deviation of MU firings in elicited contractions. Statistical data are presented as estimated marginal means with 95% confidence intervals for both the control (CON, red circles) and experimental (EXP, blue triangles) conditions. Smaller and lighter colour circles and triangles represent individual raw data points in the background.

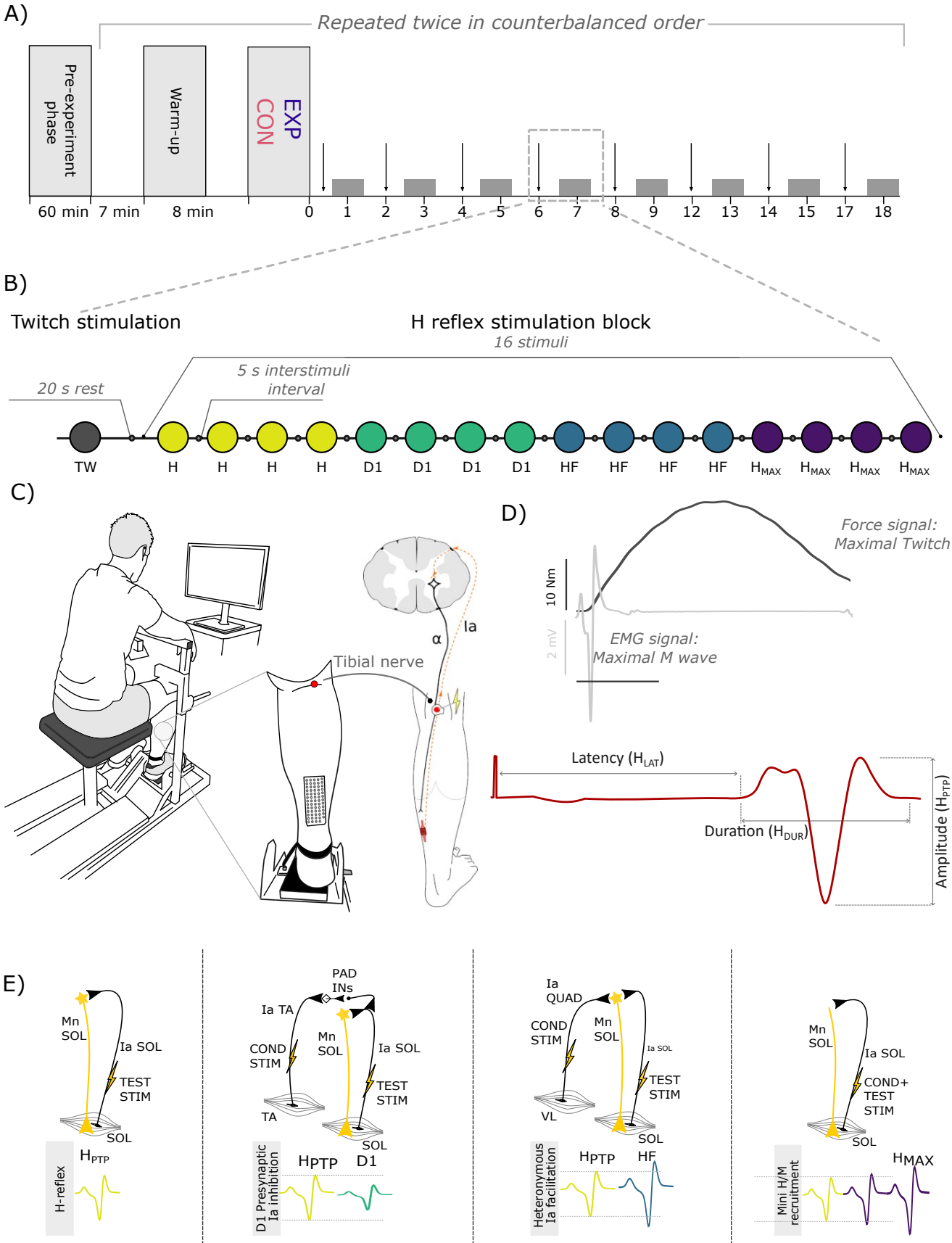

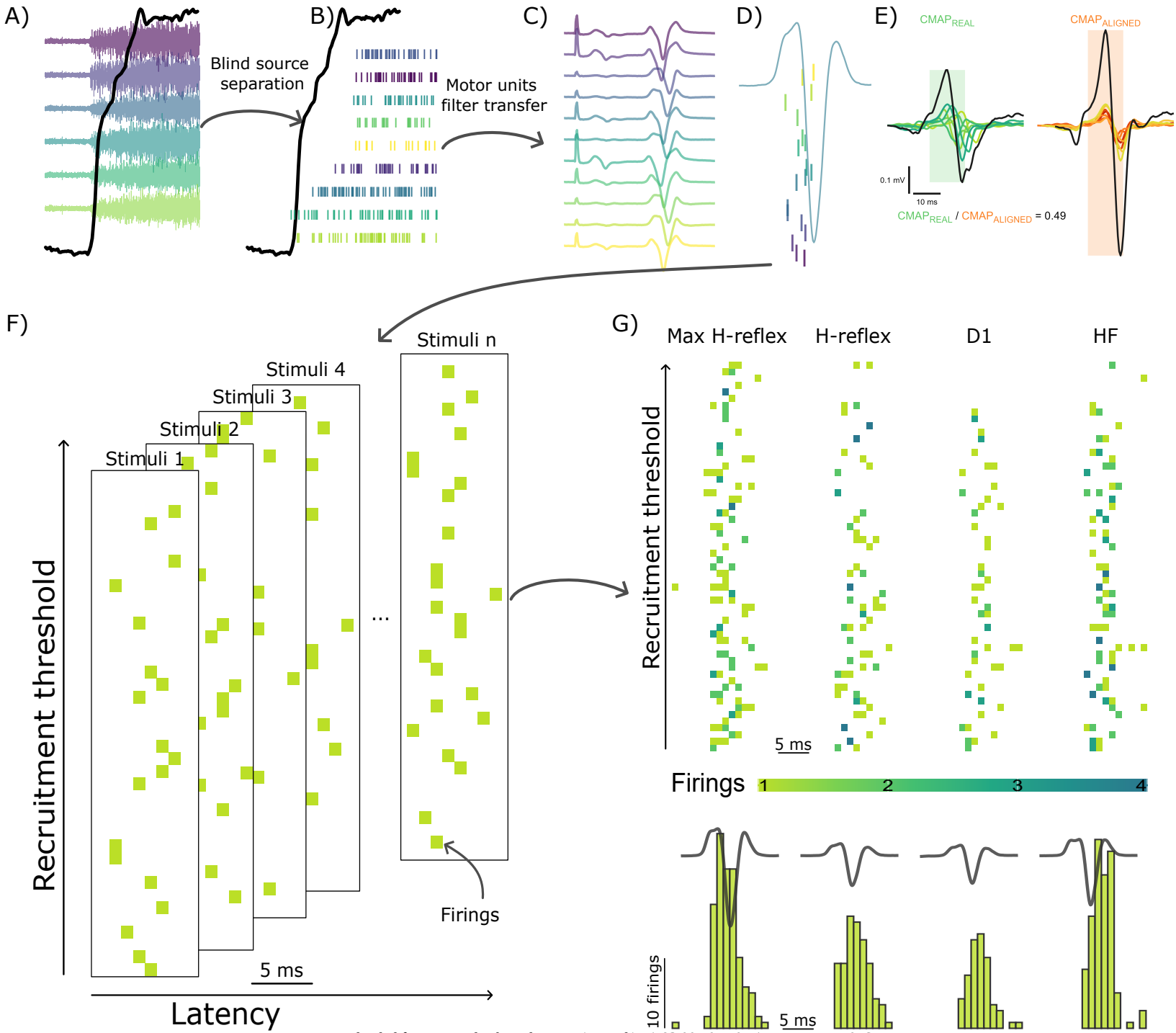

A

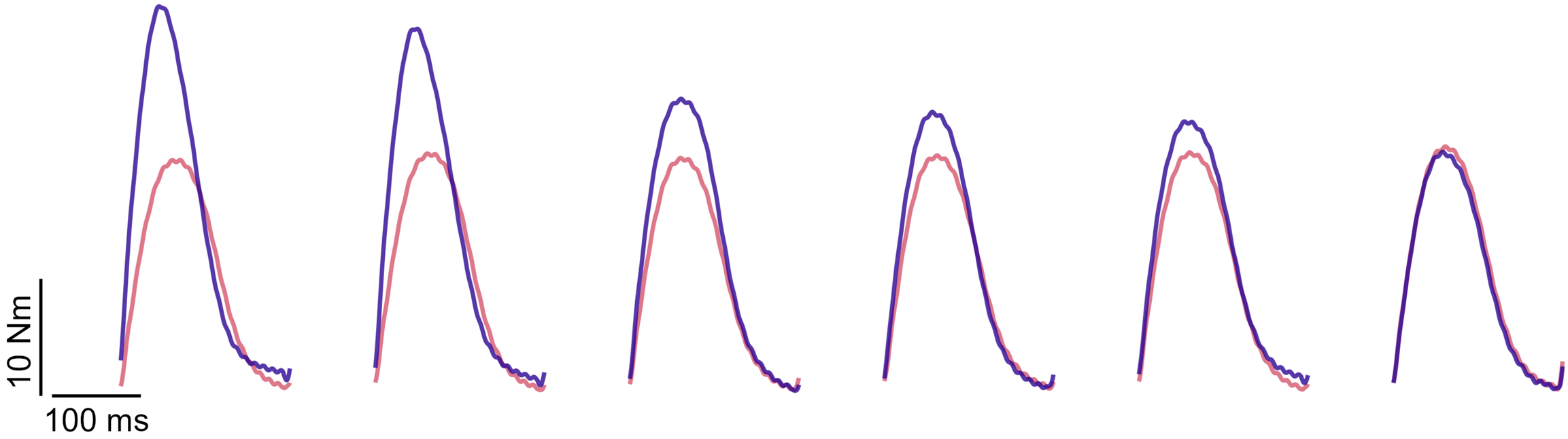

B

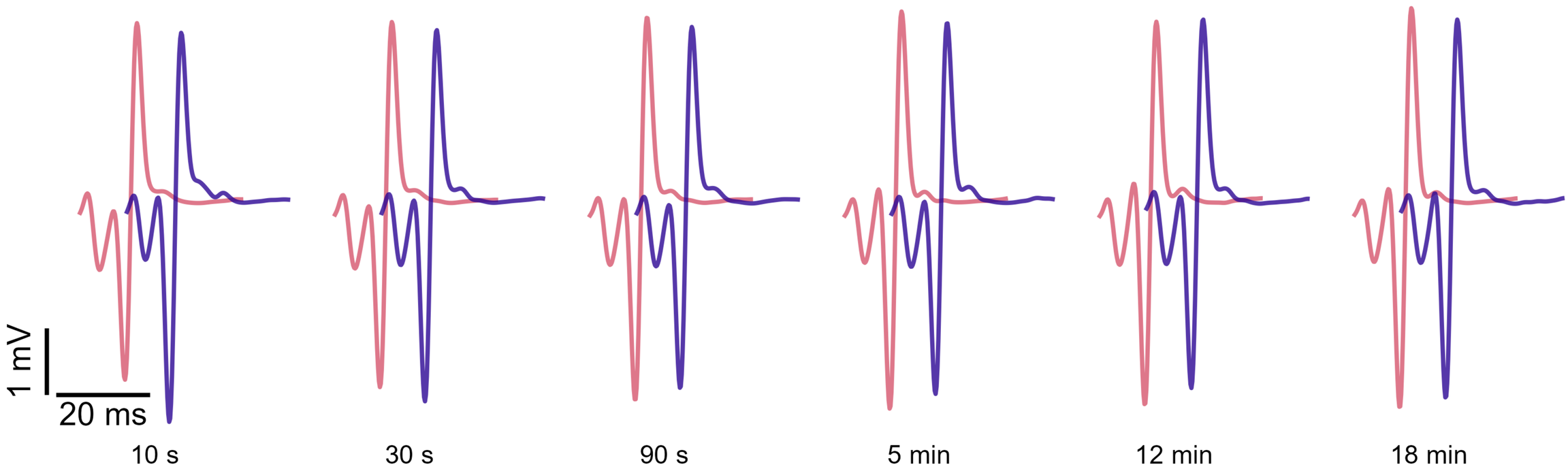

C

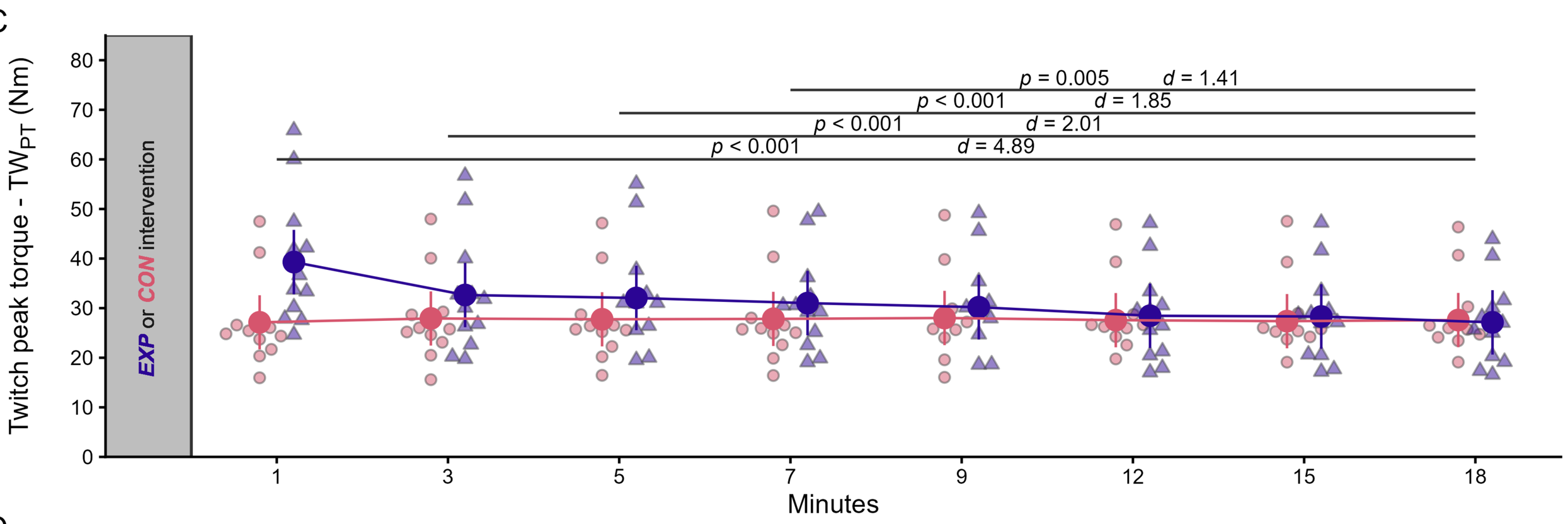

D

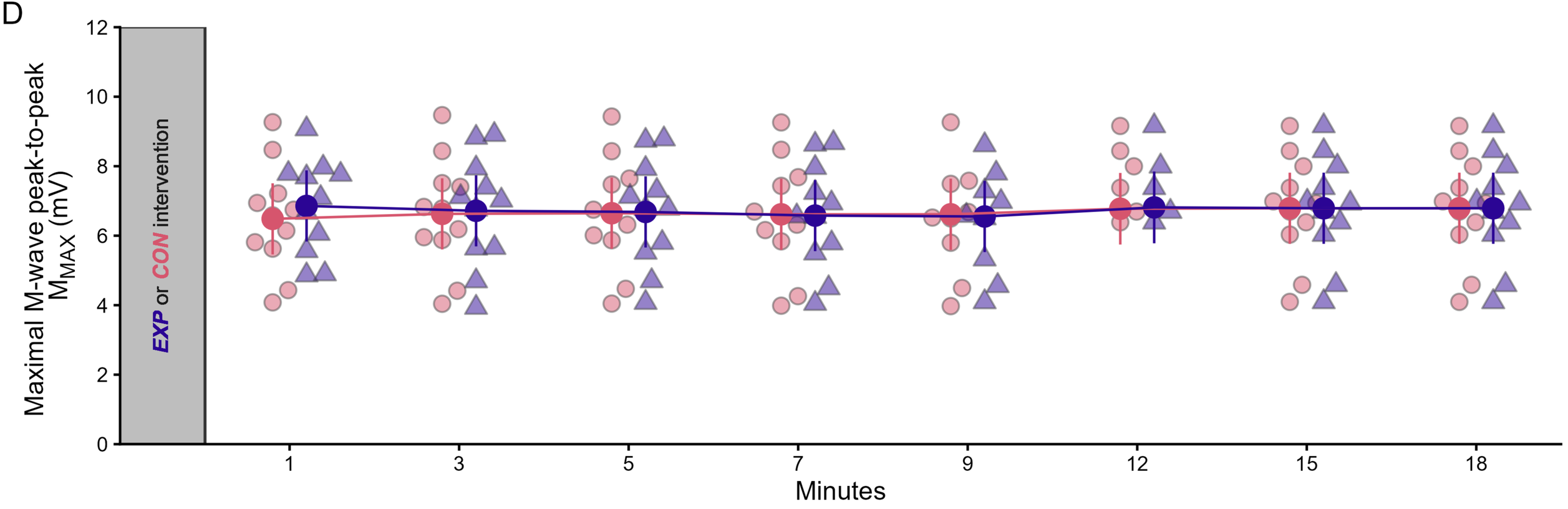

A

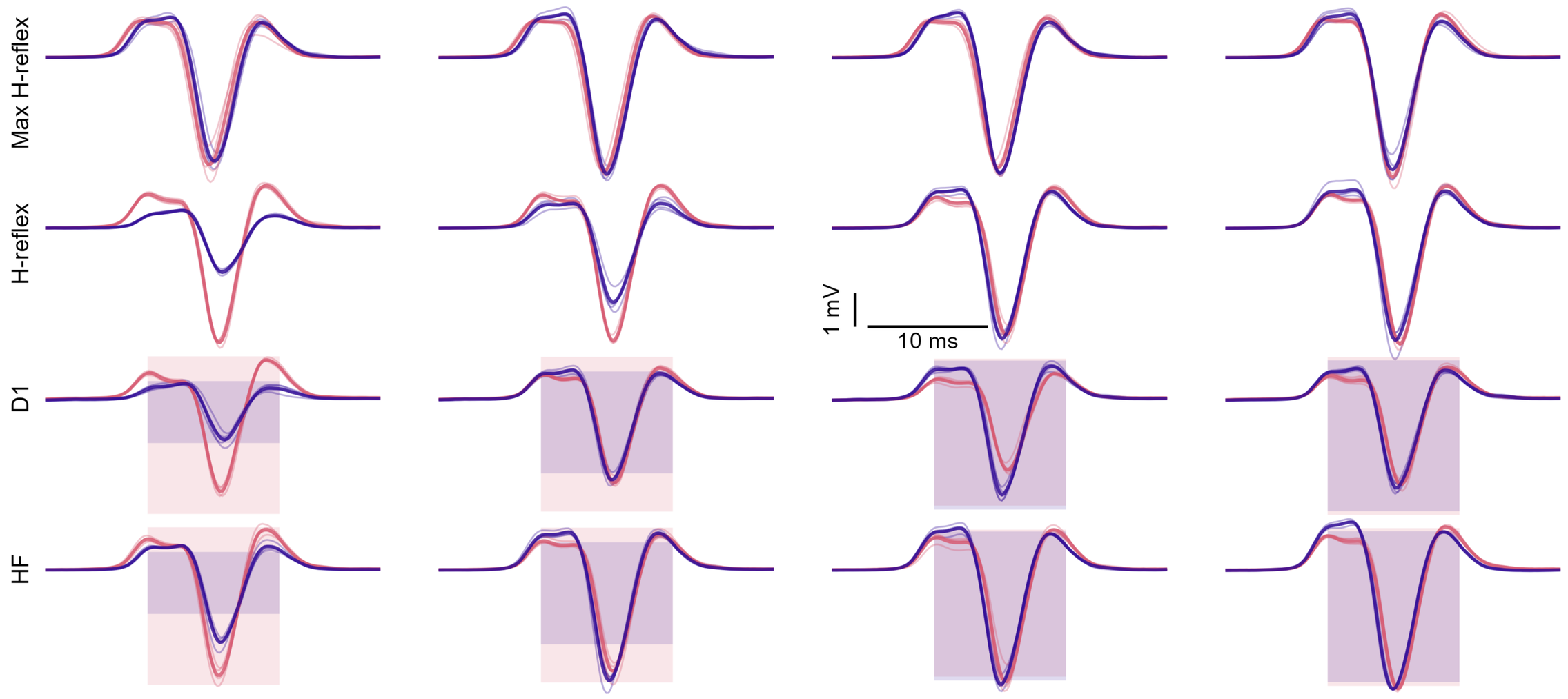

B

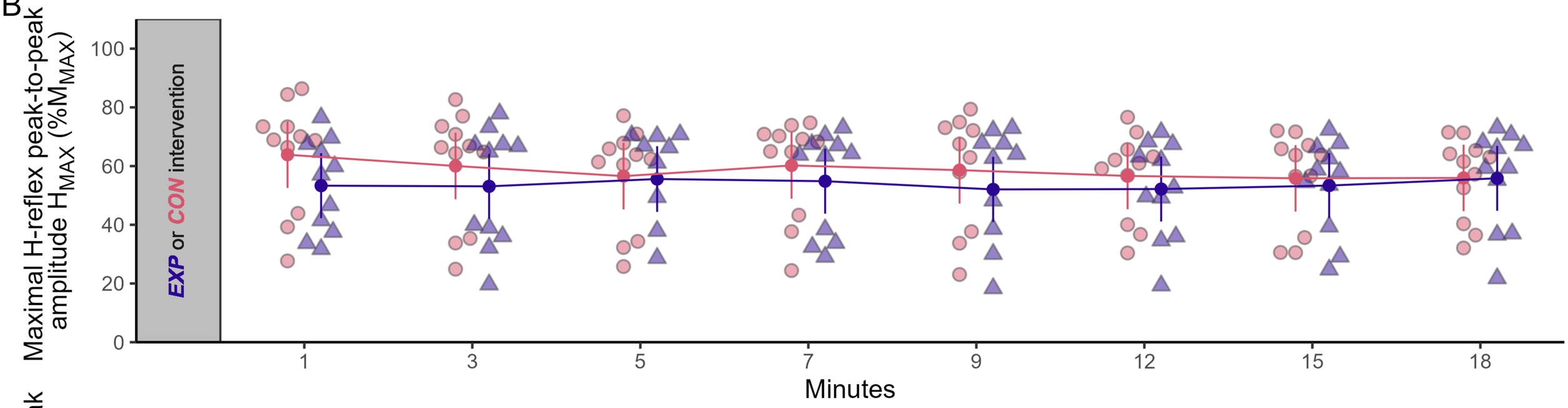

C

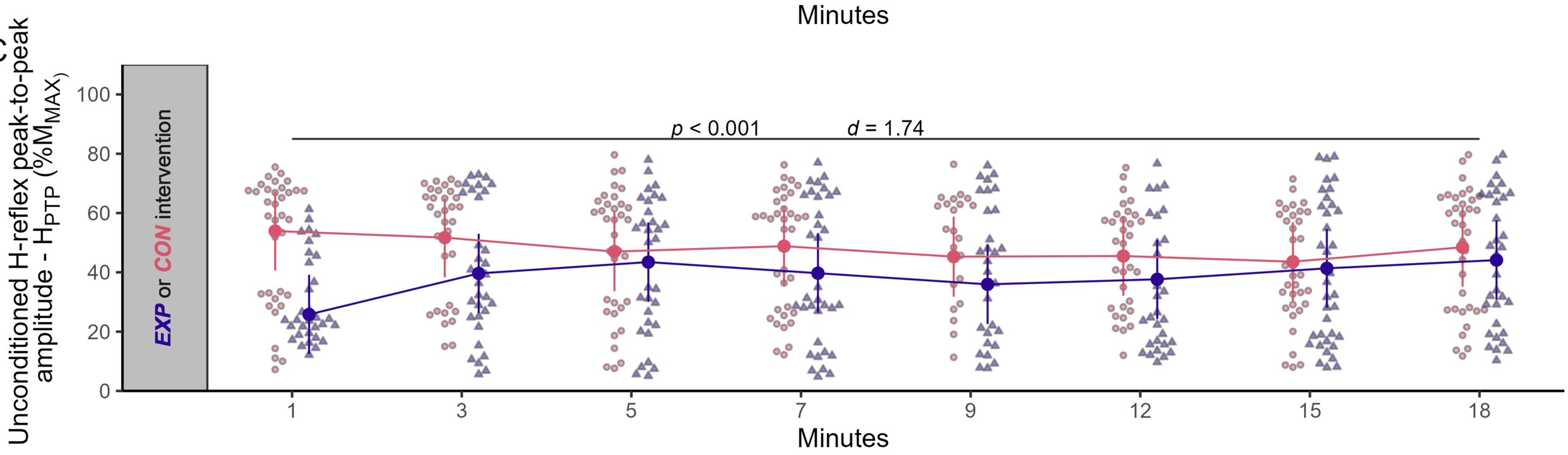

D

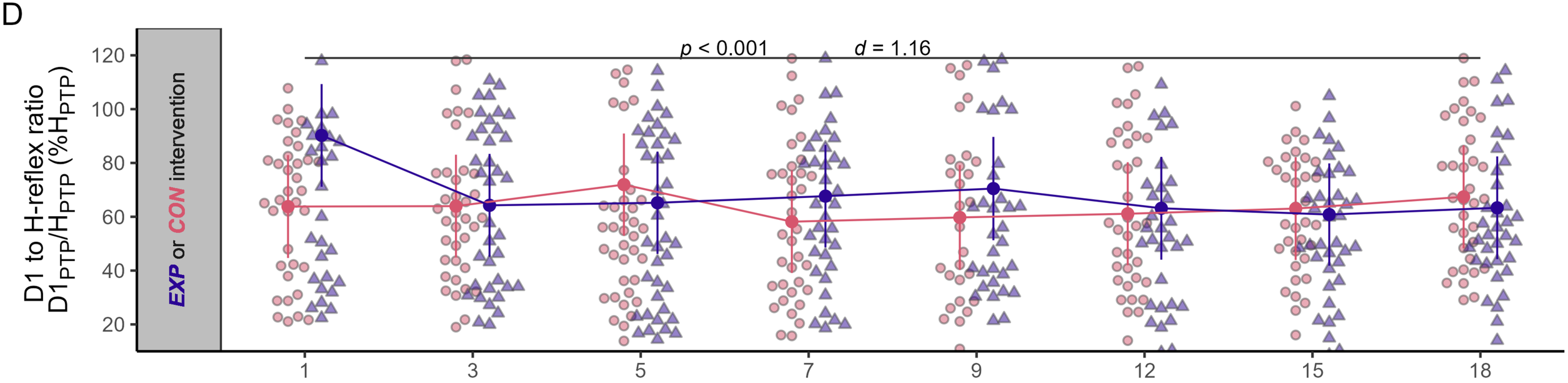

E

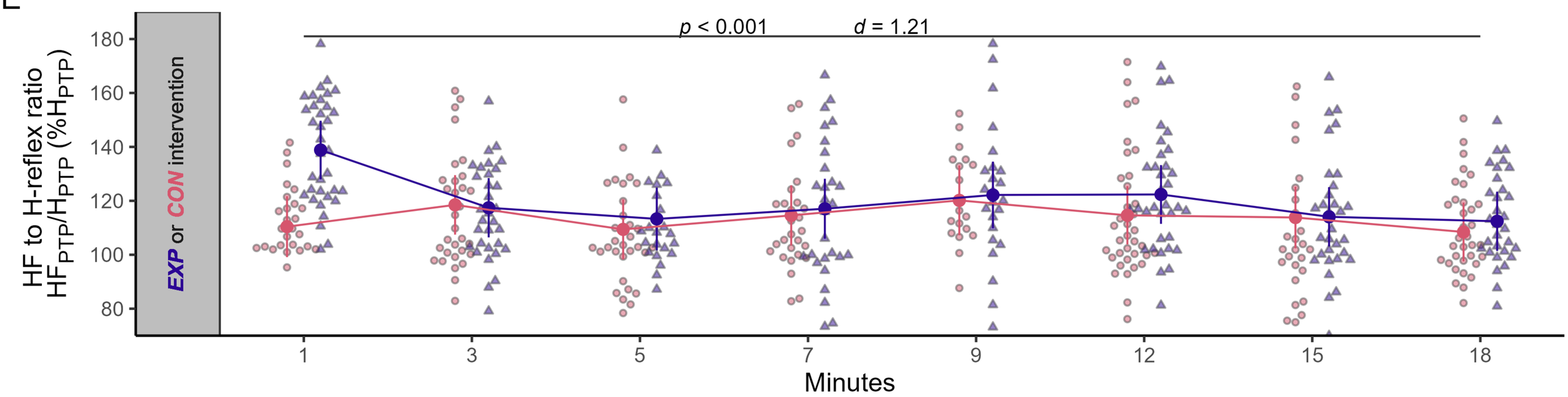

A

H
D1
HF
H_{MAX}

10ms

1 min

3 min

B

HMU_{LAT} $D1MU_{LAT}$ $HFMU_{LAT}$ $H_{MAX}MU_{LAT}$

Motor Units discharge latency (ms)

55
50
45
40
35

1 min 3 min 5 min 7 min

CON EXP

C

1 min 3 min 5 min 7 min

Motor Units discharge latency (ms)

46
45
44
43
42

HMU_{LAT}
$D1MU_{LAT}$
$HFMU_{LAT}$
$H_{MAX}MU_{LAT}$

0 20 40 60

Recruitment threshold (%MVC)

A

B

C

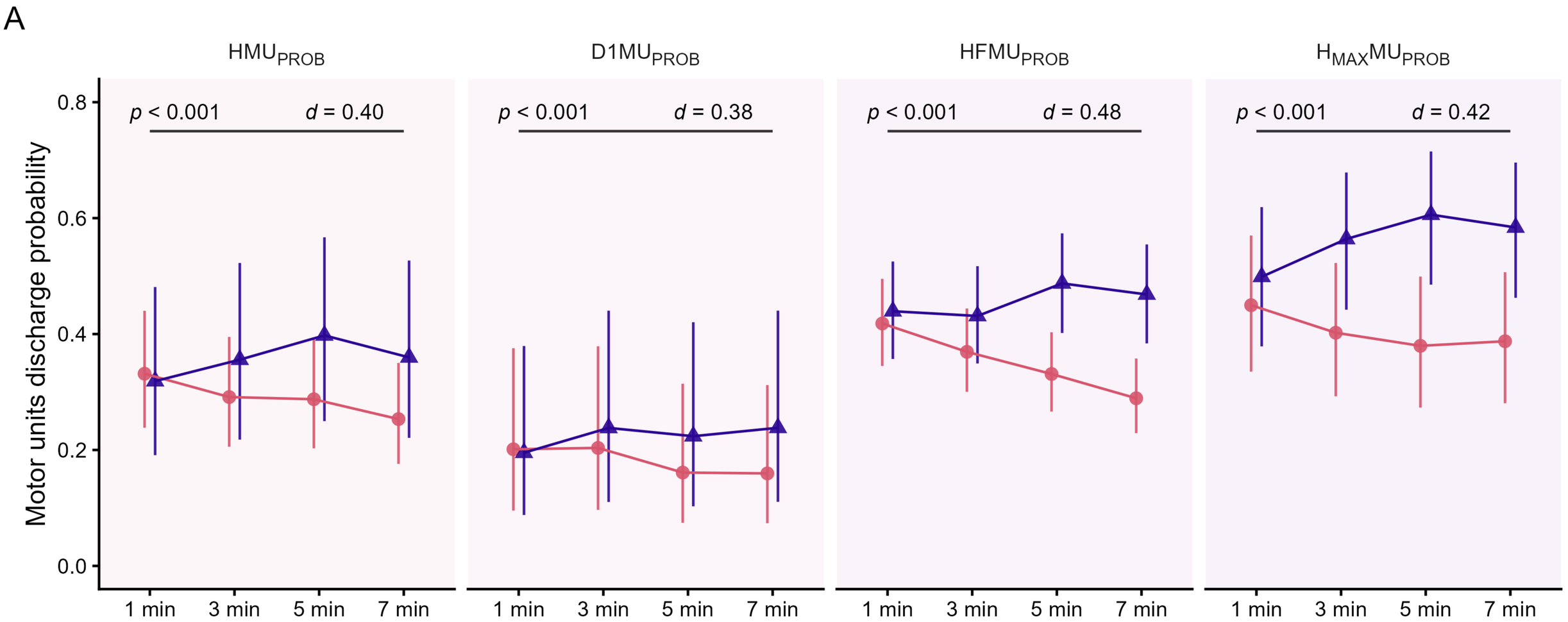

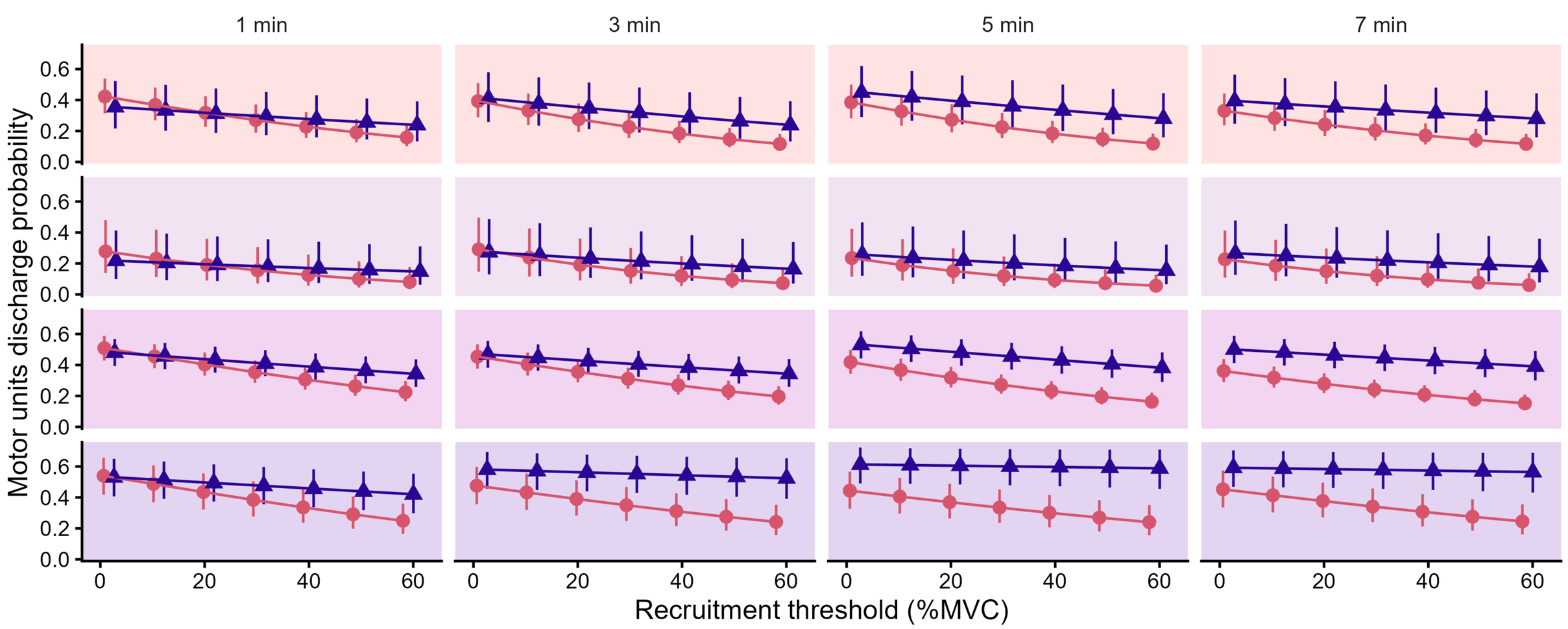

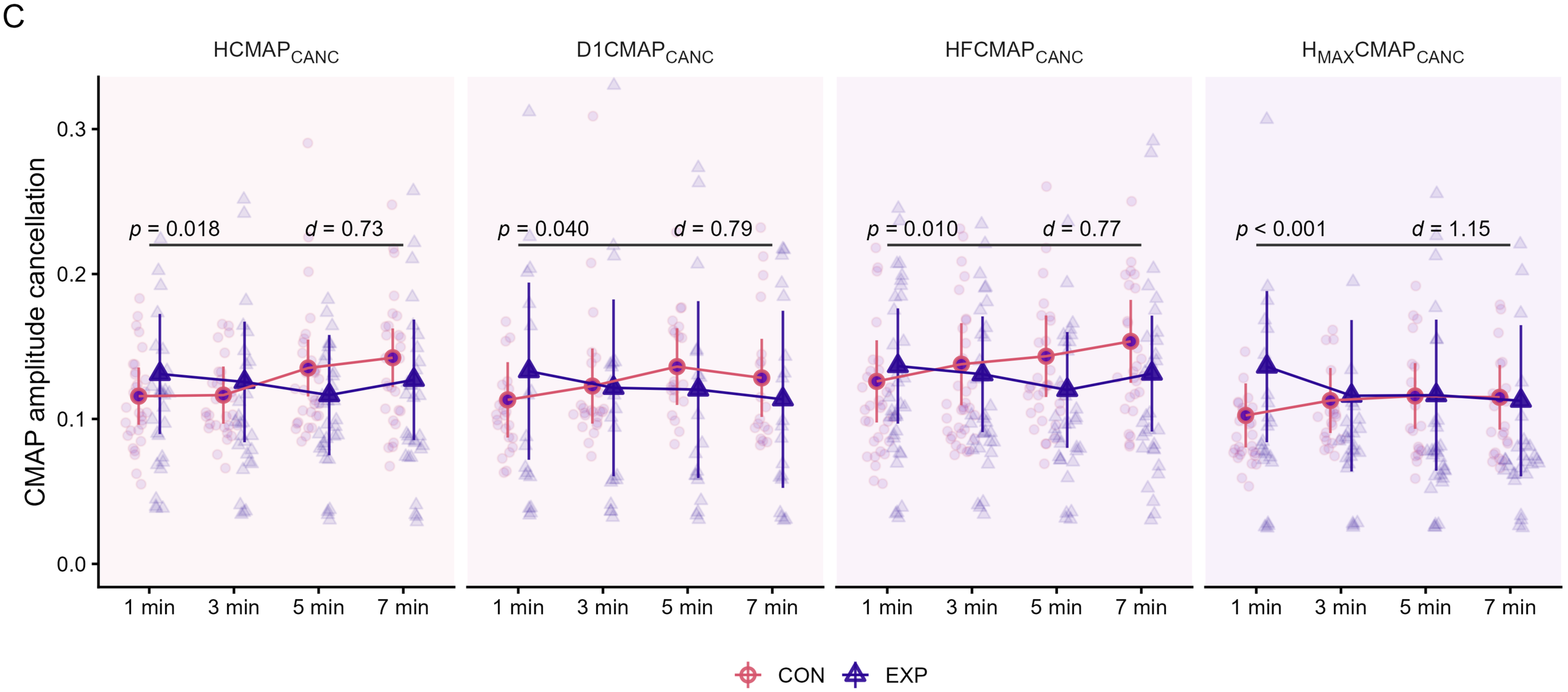

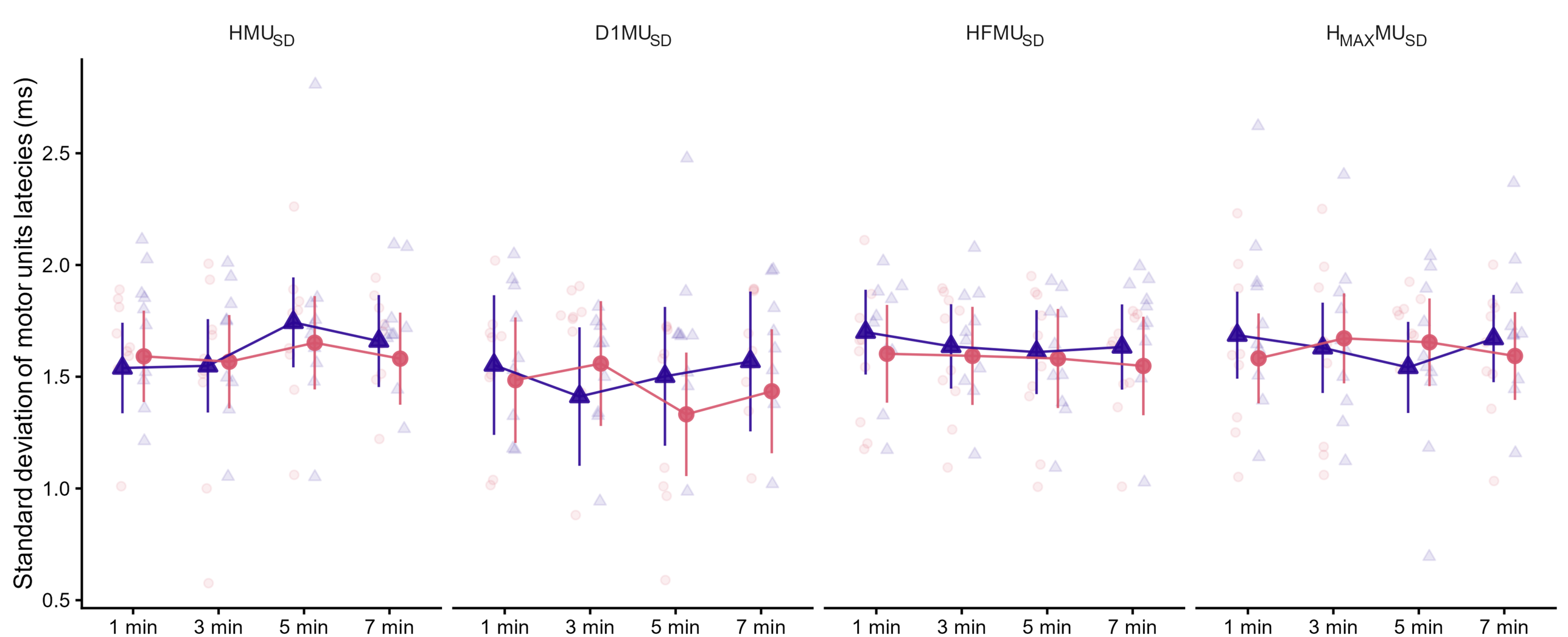

Conditioning contraction dissociates H-reflex and presynaptic spinal mechanisms

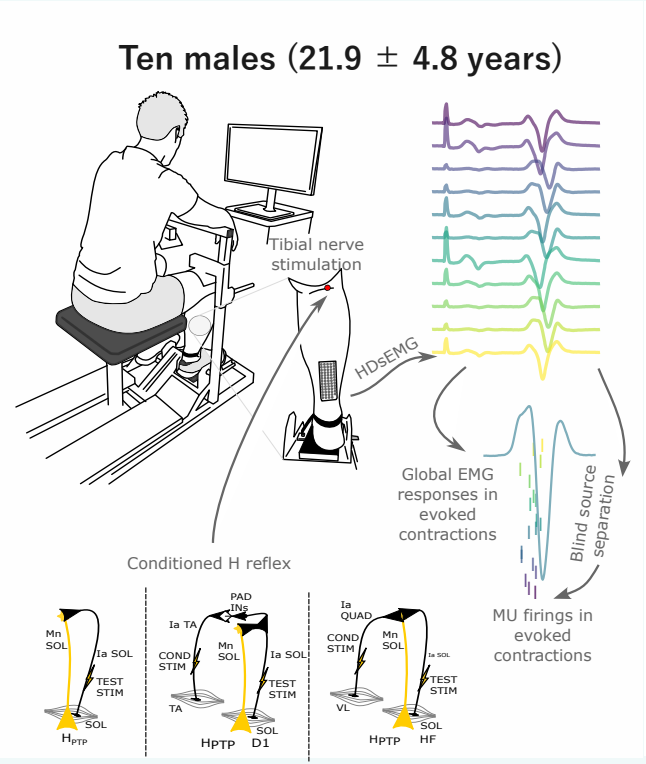

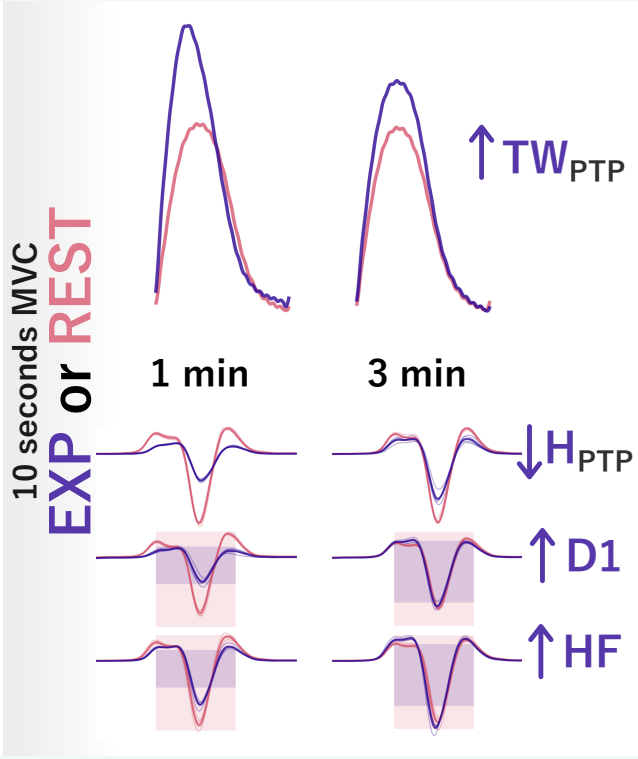

A conditioning contraction enhanced twitch torque, accompanied by a disinhibition of presynaptic inhibitory mechanisms. The concomitant reduction in H reflex amplitude suggests additional spinal mechanisms or an intrinsic muscle contraction history-dependent mechanical state may influence spinal output.